UNIVERSITY
OF OSLO

Master thesis

Investigating the potential role of circulatory extracellular vesicles in myalgic encephalomyelitis/ chronic fatigue syndrome

Elena Støvring Yran

Bioscience: Molecular Biology and Biochemistry
60 credits

Department of Biosciences
Faculty of Mathematics and Natural Sciences

May 2023

Investigating the potential role of circulatory extracellular vesicles in myalgic encephalomyelitis/chronic fatigue syndrome

Master's thesis

60 credits

Oslo University Hospital,
Department of Medical Genetics

and

University of Oslo,
The Faculty of Mathematics and Natural Sciences,
Department of Biosciences

2023

Investigating the potential role of circulatory extracellular vesicles in myalgic encephalomyelitis/chronic fatigue syndrome

Elena Støvring Yran

http://www.duo.uio.no/

Print: Graphic center, University of Oslo

Acknowledgements

This master project was conducted at the Department of Medical Genetics, Oslo University Hospital (OUS) as part of a master's degree in Bioscience: Molecular Biology and Biochemistry at the Department of Biosciences, University of Oslo (UiO).

Foremost, I would equally like to thank all the participants who contributed blood samples and demographics to this research. Thank you to CFS/ME-senteret for providing the material.

I gratefully thank my main supervisor, Marte Kathrine Viken. Thank you for including me in your research project, for expanding my knowledge, and for guiding me throughout the entirety of my stay. I deeply admire the research you conduct and how you work with your colleagues. I am very grateful to my co-supervisors, Benedicte Alexandra Lie and Anne Rydland. Thank you, Benedicte, for welcoming me into your research group and for your uplifting words and advice. Thank you so much, Anne, for patiently introducing me to the field of extracellular vesicles and new laboratory- and bioinformatic methods, and for providing the NTA- and mass spectrometry data. Thank you to my internal supervisor at UiO, Finn-Eirik Johansen, for visiting us at Ullevål, and arranging the future master's exam.

Furthermore, I would like to thank the Proteomics Core Facility, Advanced Electron Microscopy Facility, and the Department of Medical Biochemistry, all at OUS, for their contributions to the project.

Thank you to the rest of the members of the Genetics of Autoimmunity research group for inspiring me with your incredible research and talents.

Finally, I am forever grateful to my family, partner, and friends. Your support and care throughout this project have been indispensable.

Elena Støvring Yran

Oslo, May 2023

Abstract

ME/CFS is a debilitating disease thought to affect millions of individuals. Still, the etiology of ME/CFS is unknown, and there are no standard treatments or established biomarkers. The current symptom-based diagnosis is extensive, and the use of different diagnostic criteria contributes to heterogeneity among patients and may problematize the comparison of findings. Thus, the discovery of a biomarker for ME/CFS is urgent and would benefit both patients and the ME/CFS research field. Extracellular vesicles (EVs) are membrane limited vesicles secreted by all cells to the extracellular environment and can be collected through biofluids. EVs serve many functions, including transferring functional proteins, lipids, and nucleic acids between cells, thus mediating cell-to-cell communication. EV secretion and cargo may reflect disease state and EVs thus pose great potential as source of minimally invasive biomarkers.

The primary aim of this project was to study EVs in plasma from ME/CFS patients and assess the potential of EVs as source of biomarkers for the disease.

Using size exclusion chromatography, EVs were enriched from plasma from ME/CFS patients (n = 20) and healthy controls (n=20). Success of EV isolation was determined in representative patient- and control EV pools (n=5) using western blotting and transmission electron microscopy. Western blot experiments for detection of EV markers CD9, CD63 and TSG101, and albumin, were optimized and confirmed enrichment of EVs and presence of non-EV eluates in the isolated samples. EV enrichment was further validated through observation of intact EVs on transmission electron micrographs, however few CD63-positive EVs were observed. Through analysis of nanoparticle tracking analysis data, the isolated EV population primarily consisted of small EVs (< 200 nm). Within this EV population, mean- and mode EV size was similar between cohorts, but the EV concentration was significantly elevated in samples from patients compared to controls ($p = 0.006$). However, statistical tests may have been influenced by high variation within the ME/CFS cohort. Early-stage analysis of tandem mass spectrometry data identified 663 EV associated proteins. The majority of detected proteins overlapped with registered EV proteins, but only few differences could be observed between patient- and control derived samples. However, differential expression was not analyzed.

A biomarker for ME/CFS could not be suggested at this stage of the study, however increased EV concentration suggests abnormality in EV secretion in patients which strengthens their potential as source of biomarkers and further motivates EV research in ME/CFS and related diseases.

Abbreviations

AFC	Automatic fraction collector
BMI	Body mass index
BSA	Bovine serum albumin
CCC	Canadian consensus criteria
CDC/Fukuda	Centers for Disease Control and Prevention/Fukuda criteria
(D)PBS	(Dulbecco's) phosphate-buffer saline
DTT	Dithiothreitol
EBV	Epstein-Barr virus
ESCRT	Endosomal sorting complex required for transport
EV	Extracellular vesicle
F	Fraction
HC	Healthy control
HHV6	Human herpes virus 6
HLA	Human leucocyte antigens
HRP	Horseradish peroxidase
ISEV	International Society for Extracellular Vesciles
LC-MS/MS	Liquid chromatography tandem mass spectrometry
LFQ	Label free quantitation
ME/CFS	Myalgic encephalomyelitis/chronic fatigue syndrome
MHC	Major histocompatibility complex
miRNA	Micro ribonucleic acid
MISEV	Minimal information for studies of extracellular vesicles

mRNA	Messenger ribonucleic acid
NK cell	Natural killer cell
NTA	Nanoparticle tracking analysis
OUS	Oslo University Hospital
SEC	Size exclusion chromatography
sEV	Small extracellular vesicle
TBS-T	Tris-buffer saline with Tween 20
TEM	Transmission electron microscopy
TSG101	Tumor susceptibility gene 101
UiO	University of Oslo

Table of contents

Acknowledgements ..... **I**

Abstract ..... **III**

Abbreviations ..... **V**

1. Introduction **1**

1.1 Myalgic encephalomyelitis/chronic fatigue syndrome (ME/CFS) 1

1.1.1 Diagnosis and prevalence 1

1.1.2 Etiology and pathogenesis of ME/CFS 2

1.2 Extracellular vesicles (EVs) 5

1.2.1 Subtypes, biogenesis and uptake 5

1.2.2 EVs as intercellular communicators 8

1.2.3 EVs as biomarkers 10

1.2.4 Challenges in EV research 11

1.3 Prior studies on EVs in ME/CFS 12

2. Aim of study **15**

3. Materials and methods **16**

3.1 Clinical samples 16

3.1.1 Sample collection and plasma processing 16

3.2 EV isolation by size exclusion chromatography 17

3.2.1 Ultrafiltration 18

3.2.2 Software update 19

3.3 Western blotting 19

3.3.1 Lysis of EV enriched samples 20

3.3.2 Gel electrophoresis and membrane blotting 20

3.3.3 Western blot imaging 23

3.4 Transmission electron microscopy (TEM) 23

3.4.1 Negative stain- and immuno-TEM 24
3.5 Nanoparticle tracking analysis (NTA) 24
3.6 Identification of EV associated proteins by mass spectrometry 25
3.7 Statistical analyses and quality control 26
3.7.1 Analysis of patient and control demographics. 26
3.7.2 NTA data analysis 27
3.7.3 Analysis of EV associated proteins using FunRich 27
4. Results 28
4.1 Demographics of patients and controls 28
4.2 Western blot optimization 28
4.3 Successful detection of CD9, CD63, TSG101, and albumin by western blotting 30
4.4 Transmission electron microscopy confirms presence of EVs 33
4.4.1 Negative stain-TEM 34
4.4.2 Immuno-TEM 35
4.5 EV concentration and -size by nanoparticle tracking analysis 36
4.6 Proteomic profiling of EV enriched samples 39
5. Discussion 42
5.1 Is SEC an appropriate EV isolation method? 42
5.2 Can source material and processing influence results? 43
5.3 Did we enrich for EVs? 44
5.4 Characterization of sEVs in ME/CFS patients revealed difference in EV concentration but not EV size 47
5.5 An ME/CFS specific sEV protein profile was not identified 49
5.6 Assessment of circulatory EVs as a source of potential ME/CFS biomarkers 49
5.7 Considerations for future studies 50
6. Conclusion 52
References 53

Appendix 1. Antibodies **61**

Appendix 2. Software **63**

Appendix 3. Histograms and Q-Q plots of NTA data **64**

1. Introduction

1.1 Myalgic encephalomyelitis/chronic fatigue syndrome (ME/CFS)

Myalgic encephalomyelitis/chronic fatigue syndrome (ME/CFS) is a complex, multifactorial disease of unknown etiology and pathogenesis with no established biomarker or standard therapeutic approach (1-3). ME/CFS is characterized by core symptoms of "post-exertional malaise" following physical, mental or social activity, persistent debilitating fatigue not relieved by rest, cognitive impairment described as "brain fog" and non-refreshing sleep with additional symptoms including chronic pain, gastrointestinal issues, sensory hypersensitivity, orthostatic intolerance, frequent flu-like infections, and other symptoms related to dysfunction of the immune- and nervous system (1-5).

ME/CFS patients are a heterogenous group experiencing the aforementioned, and other, symptoms to a varying degree. Cases of ME/CFS range from mild, in which the patient is able to moderately partake in social life, education and/or work, to severe cases in which the patient is bedridden and reliant on full-time assistance, often by family members, for life-sustaining tasks such as eating or drinking (3, 4). ME/CFS is a debilitating disease that gravely reduces the patients' function and quality of life compared to pre-onset, and it is a major public health- and economic problem (2, 6).

ME/CFS is an unusually debated disease that is still met with misconceptions and skepticism, even from health care professionals (5, 7). An extensive review of literature on ME/CFS conducted by the Committee on the Diagnostic Criteria for Myalgic Encephalomyelitis/Chronic Fatigue Syndrome by the Institute of Medicine, Washington, DC, concluded that ME/CFS is a medical physiological illness, not psychiatric or psychological (7).

1.1.1 Diagnosis and prevalence

Diagnosis of ME/CFS is elaborate due to symptom overlap with other diseases and the lack of diagnostic biomarkers (1, 5). Currently, diagnosis is based solely on the patient's symptoms coupled with ruling out other possible causes of the symptomatology (2, 5). There has been

identified close to 20 different case definitions used for ME/CFS diagnosis (8). Within ME/CFS research, the 1994 Centers for Disease Control and Prevention/Fukuda Criteria (CDC/Fukuda) (9) has been the most used (2), followed by the 2003 Canadian Consensus Criteria (CCC) (10) and its sequel, the 2011 International Consensus Criteria (11). They differ in their inclusion- and exclusion criteria which adds to the heterogeneity among ME/CFS patients. This is thought to contribute to the contradictory results and differences in reported prevalence of ME/CFS between studies (12). This is illustrated in the systematic review and meta-study performed by Lim et al. of 56 sets of prevalence data from 46 studies in which the prevalence of ME/CFS ranged from 0.01% to 7.62%, with case definition and diagnostic methods being the most influential factors (12). The meta-analysis of their entire dataset reported a prevalence of 0.68% (95% CI: 0.48–0.97) (12). However, this might be an overestimate considering the majority of the prevalence datasets used in the meta-analysis were from studies that used the CDC/Fukuda case definition (12). This case criteria is frequently criticized for being overinclusive (2), and reported overall higher prevalence than the studies that used another group of case definitions including the CCC (12).

ME/CFS onset can start at any age but most frequently occur in the teens or thirties (13, 14). Prevalence is commonly reported to be higher in women, ranging from being 1.5-fold (12) to above 4-fold (15) higher than in men. However, there is discussion on whether this is the true ratio or caused by sampling-bias and underdiagnosis of men (1, 2).

1.1.2 Etiology and pathogenesis of ME/CFS

ME/CFS etiology and pathogenesis is not understood, but several hypotheses on their respective mechanisms have emerged within the ME/CFS research field during the past few decades. The central hypotheses include abnormalities within metabolism, genetics, the endocrine-, vascular-, immune-, and nervous system. The possibility of subgroups within the disease has also been proposed. This section will mostly elaborate on the hypotheses related to immune function, as they are the most relevant to this thesis' underlying hypothesis of ME/CFS being an immune-mediated disease.

Genetic predisposition

ME/CFS is believed to be multifactorial, influenced by both genetic- and environmental factors. The hypothesis of a genetic predisposition to ME/CFS is supported by a study of 811 patients in which it was observed a significantly increased risk ratio of ME/CFS for first- (risk

ratio = 2.70), second- (risk ratio = 2.34) and third-degree relatives (risk ratio = 1.93) (16). The maintained significance in second- and third-degree relatives (p=0.008 and p=0.009) strengthens the possibility of a heritable disposition, by diminishing the effects from shared lifestyle and environment between close relatives. Twin studies on chronic fatigue have shown the concordance of chronic fatigue in both individuals within a pair to be higher in monozygotic than dizygotic twins (17, 18). Supporting both the hypothesis of a genetic predisposition and the involvement of the immune system, several studies, some of which were conducted in Benedicte A. Lie's research group, indicate an association between specific human leukocyte antigen (HLA) alleles, both class I and II, and ME/CFS (19, 20)

Infection as potential trigger

The most commonly reported trigger of ME/CFS onset is infectious diseases (14). Several pathogens are thought to be linked to onset of ME/CFS, in particular the immune-cell-targeting herpesviruses human herpes virus 6 (HHV6) and Epstein-Barr mononucleosis virus (EBV) (21-24). It has been suggested that immune dysregulation in ME/CFS patients may be caused or worsened by viral infections, resulting in a chronically activated dysfunctional immune system, persistent infection, reactivation of latent viruses and autoreactivity (22). However, these viruses are commonly detected in healthy individuals. Thus, it is likely that disease triggering would require a predisposition in patients causing insufficient viral clearing or abnormally acute infection to allow the further immune dysregulation (22). A recent serological study saw only a slightly higher level of persistent infection by HHV6 in patients than controls, but significantly higher frequency of persistent active phase infection of HHV6 in patients (25). In addition, patients with active phase infection had higher levels of both pro- and anti-inflammatory cytokines than patients with latent phase infection (25). The hypothesis could further be supported by a prospective study that followed more than 200 participants over 12 months after confirmed infection by either EBV, Q fever or Ross River virus that found severity of acute sickness during infection to be predictive of the risk of developing post-infective ME/CFS (26).

Immunological and autoimmune etiologies

Several symptoms support the hypothesis of ME/CFS being an immune-mediated disease including frequent infections, inflammation, and flu-like symptoms without presence of pathogens (1). It has been demonstrated differences in the immune cell signature of ME/CFS patients compared to healthy controls, particularly regarding subpopulations of natural killer

cells (NK cells), T cells and B cells (27, 28). A study of elderly ME/CFS patients showed that they were at a moderately higher risk of B-cell lymphomas, implying frequent B-cell activation (29). Furthermore, several studies report reduced NK cell cytotoxicity and altered -cytokine production in ME/CFS patients (27, 30, 31). However, some studies did not corroborate these differences in lymphocyte phenotype and cytotoxicity (32).

The possibility of an autoimmune etiology to ME/CFS has gained support following studies that showed symptom improvement in some patients following prolonged CD20 positive B-cell depletion therapy using rituximab (33, 34). The clinical response occurred months after starting the B-cell depleting therapy. Fluge et al. hypothesized the improvement in patients to be caused by lower levels of autoantibody-producing plasma cells, following the depletion (33, 34). However, these effects could not be reproduced in their double-blind study (35). Elevated levels of certain autoantibodies in ME/CFS patients have previously been documented by several studies (36, 37), and another study showed that removal of autoantibodies against β2-adrenergic receptors improved the condition of the majority of included patients (38). Loebel et al. later observed a decline of autoantibody levels in B-cell depleted patients (37).

Furthermore, Fluge et al.'s ME/CFS cohort had a high frequency of first-degree relatives with autoimmune diseases (41%), which is relevant due to previously observed familial aggregation of autoimmunity (34, 39). ME/CFS share other traits with autoimmune diseases, including the previously mentioned female predominance and HLA associations. Furthermore, several autoimmune diseases that share symptoms with ME/CFS are also thought to have EBV infection as a risk factor including multiple sclerosis, rheumatoid arthritis, systemic lupus erythematosus, and autoimmune thyroid diseases (40, 41).

Taken together, these studies hint at a possible dysregulation of the immune system in at least a subgroup of ME/CFS patients. This might cause inflammation of the central nervous system or dysregulated blood flow causing tissue hypoxia and could describe why patients experience such a broad variety of symptoms (3, 42). Still a lot more research on the pathology of ME/CFS is needed. The discovery of a diagnostic biomarker would contribute to higher quality research through more accurate and efficient diagnosis of the ME/CFS participants.

1.2 Extracellular vesicles (EVs)

Extracellular vesicles (EVs) are small, non-replicating, membrane limited vesicles secreted by cells into the extracellular space (43-46). Most cells are thought to be capable of secreting EVs (47, 48), a phenomenon evolutionarily conserved from prokaryotes to eukaryotes, including plants (43). EVs carry a diverse cargo from their donor cell that can consist of proteins, RNA, DNA, lipids, cytokines, and metabolites (45, 48, 49). The EV composition depends on the type and state of the donor cell (50). After secretion, EVs can transfer functional cargo from their donor cell to a recipient cell, potentially modifying the recipient cell's phenotype and thus contributing to cell-to-cell communication (50). In this way, EVs are significant in several physiological and pathological processes and show great potential for use in therapeutics and as biomarkers (43-45, 47, 48, 51, 52).

EVs were established as functional biological entities through research conducted in the 1980s and -90s, and EV research has been rapidly growing since the year 2000 (53). In 2011 prominent EV researchers established the International Society for Extracellular Vesicles (ISEV) with goals to connect, guide, and advance the rapidly expanding EV research field (53, 54). In 2014, ISEV published a list of minimal information for studies of extracellular vesicles (MISEV) (55), a proposed guideline for the research field which was updated in 2018 (MISEV2018) (46).

1.2.1 Subtypes, biogenesis and uptake

As of today, EVs are commonly divided into three main subgroups based on their biogenesis namely apoptotic bodies, microvesicles and exosomes (43, 56) (see Figure 1).

Apoptotic bodies

Apoptotic bodies, also termed apoptotic blebs, apoptosomes or apoptotic microvesicles, is the subgroup of EVs most heterogenous in size, with reported diameters ranging from 50 nm to 5 µm, though more commonly reported as large EVs (56-58). Apoptotic bodies are shed from the plasma membrane of cells undergoing apoptotic cell disassembly, after the plasma membrane delaminates from the cytoskeleton due to increased hydrostatic pressure, causing membrane blebbing (57-59). Thus, a unique trait of apoptotic bodies in comparison to EVs of other subtypes is that their cargo can consist of chromatin pieces and fragmented or whole organelles (60).

Microvesicles

Microvesicles, often referred to as ectosomes, microparticles or shedding vesicles, are also formed by the outward budding and fission of the plasma membrane, but of viable cells (43, 45, 56, 61). Their diameter are described as between 100 nm to 1000 nm (48, 62). The biogenesis of microvesicles is not as well understood, however, microvesicle secretion occurs during normal cell state and can change as a response to stimuli of the donor cell (43, 57).

Exosomes

Exosomes are the most studied of the three subgroups and are of specific interest due to the assumed specific sorting of their cargo (63). They are smaller EVs of endosomal origin with diameter range of 30 to 150 nm (48, 64). Their biogenesis begins with the inward budding of the limiting membrane of an early endosome maturing into an multivesicular body; a late endosome containing several intraluminal vesicles (44, 51, 65) (see Figure 1). Intraluminal vesicle formation starts with the translocation of transmembrane tetraspanins, a protein superfamily, into tetraspanin enriched microdomains on the endosomal membrane (52). Further biogenesis may rely on the recruitment of the “endosomal sorting complex required for transport” (ESCRT) and ESCRT-accessory proteins, to form the intraluminal vesicles and specifically sort cytosol, proteins, nucleic acids and other cargo to the formation site (44, 65). The mature multivesicular bodies are either destined to fuse with lysosomes, resulting in degradation of their content by lysosomal hydrolases, or fuse with the plasma membrane subsequently releasing their intraluminal vesicles into the extracellular space, which upon exiting the cell are termed exosomes (44, 51, 58, 64). Furthermore, ESCRT-independent exosome biogenesis has been documented (66), which is thought to occur through several pathways including dependence on tetraspanins (52, 67). However, in line with ESCRT-dependent biogenesis, ESCRT-independent exosome biogenesis is not thoroughly understood (52).

Considering exosome biogenesis, endosomal tetraspanins (e.g. CD63, CD9 and CD81), other endosomal proteins (e.g. HSC70) and ESCRT- and accessory proteins (e.g. TSG101 and Alix) are thought to be enriched in exosomes and are commonly used as general EV markers to validate presence of EVs in samples (46, 52, 68).

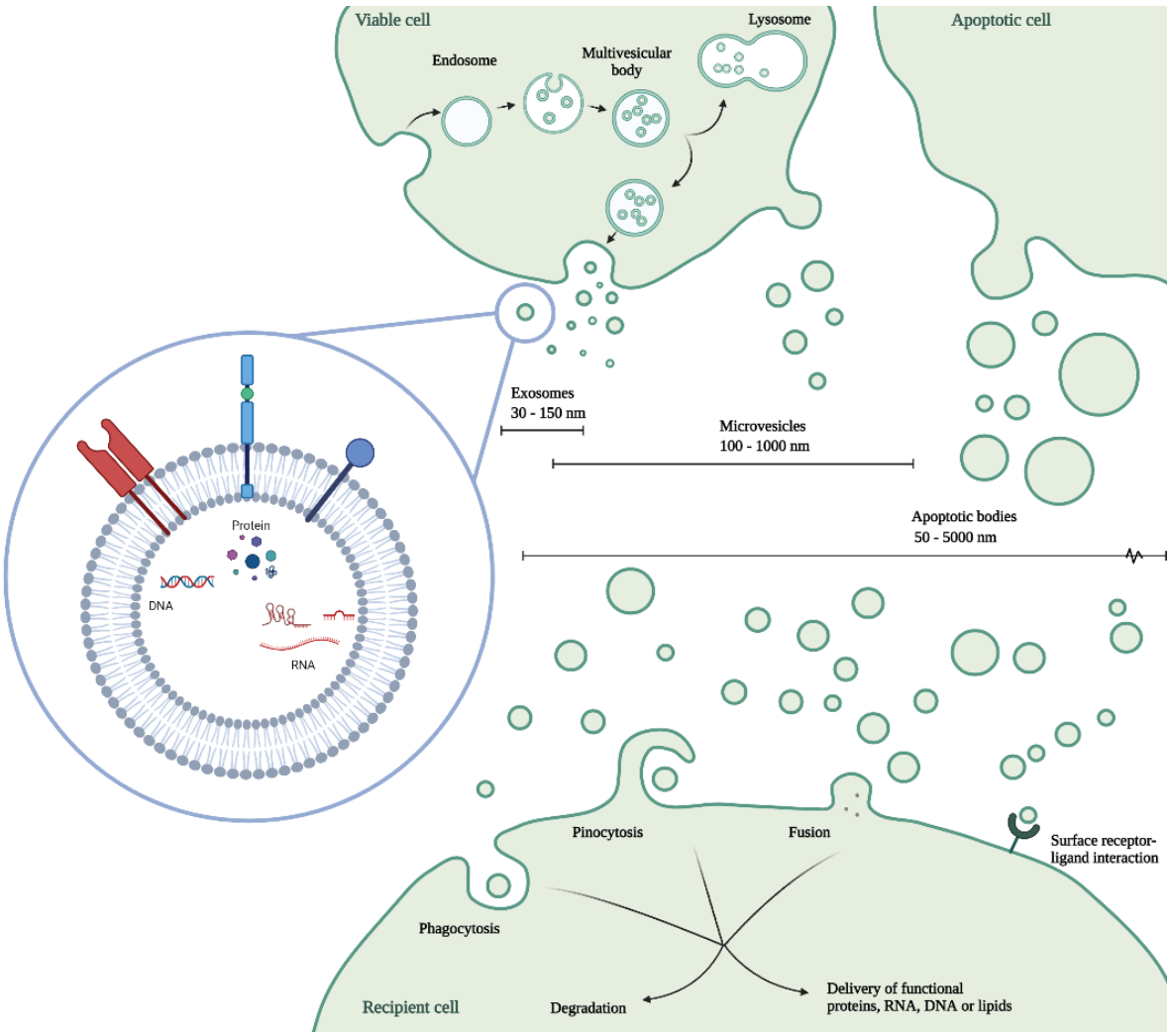

Figure 1: Extracellular vesicles (EVs) mediate cell-to-cell communication. EVs are divided into three subgroups based on biogenesis namely apoptotic bodies, microvesicles and exosomes. EVs are membrane limited vesicles secreted by cells into the extracellular space and carry various cargo including nucleotides, proteins, and lipids. EVs may transfer this functional cargo to a recipient cell, thus mediating intercellular communication. Figure created in Biorender.com, inspired by references (44, 45).

The subgroups are often accompanied by size- and suggested protein markers, yet it is currently difficult to distinguish the subgroups after secretion (43, 46). The nomenclature, size range and classification of EVs is controversial, and the use and definitions of EV subgroups varies within the literature making it important for each writer to state the definition they are using (46, 69). Even the terms themselves have changed meaning during the development of the EV research field (69). Like other aspects of the EV research field, classification and nomenclature of EVs lacks standardization and consensus. Considering this, as well as the lack of definitive markers to distinguish EV subtypes after secretion, it is advised to use

"EVs" as the general term for all secreted vesicles (43, 46, 69). The term can alternatively be accompanied by physical traits like size, density, or biochemical composition (46).

Uptake and interaction

The EVs' target, functionality, and way of interaction with the recipient cell and extracellular components depends on the EVs' characteristics including size, lipid composition, cargo and surface molecules including receptors, ligands and adhesion molecules (70). EVs transfer information to the recipient cell using different mechanisms. Receptor-ligand interaction between the EV- and recipient cell's surface may trigger intercellular signaling pathways in the cell (71). Furthermore, functional EV cargo can be delivered to the target cell, which if not degraded may affect the recipient cell's phenotype. Cargo delivery occurs either through fusion of the EV membrane with the cell membrane, or through internalization of the EVs by clathrin mediated or -independent endocytosis, phagocytosis or macropinocytosis (43, 72) (see Figure 1). The depiction of EV uptake and cargo delivery mechanisms, including the degree of target specificity, is incomplete (50).

In addition to enclosed and transmembrane cargo, proteins and -complexes may coat the EV surface upon secretion, referred to as the EV protein corona (73). The EV corona is not well explored but is believed to contribute to the function of EVs (73, 74). Furthermore, EVs may specifically associate with other extracellular components e.g. immunoglobulins, complement factors, cytokines, lipoproteins and enzymes (75).

1.2.2 EVs as intercellular communicators

Secretion of EVs was initially described as a route for cells to dispose of unwanted compounds (65). In 1987, Johnstone et al. studied EVs derived from sheep erythrocyte culture, and suggested that secretion of EVs was utilized by the reticulocytes to shed membrane proteins during their maturation to erythrocytes (76). Removal of unwanted cell components is one way in which EVs contribute to homeostasis, however it has since then been revealed that EVs play an integral role in how cells communicate with other cells and their extracellular environment. Interest in EVs as cell-to-cell communicators increased following discoveries in 2006-2008 of EVs transferring functional messenger RNAs (mRNAs), micro RNAs (miRNAs), and proteins between cells (77-79). These three studies all observed that mRNAs from EVs were translated in the recipient cell, and that specific RNAs and/or proteins were strongly enriched in the EVs compared to their donor cells, hinting at

specific sorting of their cargo (77-79). Recently, the primary interest in EVs is in their ability to transfer both enclosed and exposed cargo between cells, and how this can be applied in therapeutics and diagnostics (43-45, 51, 80).

EVs are involved in a vast multitude of both physiological and pathological processes (43), including cardiovascular homeostasis (81), coagulation and thrombosis (82), cell-free antigen presentation (83), reproduction (84), tumor progression (51), inflammation and immune function (85), among others. In the central nervous system, glial cell derived EVs help maintain its homeostasis, regulate neurons and mediate neuroprotection (86). EVs can cross the blood-brain barrier bidirectionality and are thus also communicators between the central nervous system and the periphery (87, 88). Furthermore, EVs are also shown to contribute to the pathology of several neurodegenerative and -inflammatory diseases including Alzheimer's and Parkinson's disease (88, 89).

EVs and the immune system

EVs are secreted by all immune cells and are involved in both immune stimulatory and -suppressive mechanisms (85). The interest in EVs' involvement in the immune system grew following the discovery made in 1996 that EBV infected antigen-presenting cells secreted EVs enriched in EBV proteins and major histocompatibility complex (MHC) proteins, and that these were capable of presenting antigens to activate T cells (83). Since, EVs derived from other cell types have been suggested to be capable of antigen presentation. Recently, a subgroup of platelet-derived EVs were found to have enrichment of 20S proteasomes, MHC-I, and lymphocyte costimulatory molecules CD40L and OX40L (90). The proteasome degraded proteins into smaller peptides for presentation by the MHC-I molecule which induced T-cell proliferation (90).

The role of EVs in immunosuppression has predominantly been studied in the context of cancer. One proposed technique of tumors using EVs for immune evasion and suppression is using EVs as decoys. Secreted tumor-derived EVs have been observed to decrease cytotoxicity of NK- and cytotoxic T-cells through expressing transforming growth factor β and ligands to their stimulatory receptor, NKG2D, resulting in lower expression of the receptor thus impairing their function (91, 92). Moreover, cancer cell-derived EVs have been shown to induce apoptosis in CD8+ T cells (93), induce polarization of surrounding tumor associated macrophages to the pro-tumorgenic M2 phenotype (94) and initiate pre-metastatic niche formation (95).

EVs are also implicated in the immunopathology of several autoimmune diseases (96). They present autoantigens and can therefore trigger autoreactive immune responses (96). For instance, in the synovial fluid of rheumatoid arthritis patients EVs have been shown to carrying citrullinated proteins, known rheumatoid arthritis-specific autoantigens, that are recognized by antibodies and form inflammatory EV-associated immune complexes (97, 98). One study incubated peripheral blood mononuclear cells with serum EVs from systemic lupus erythematosus patinets and healthy controls, in which patient derived undisrupted EVs induced stronger production of proinflammatory cytokines (99).

1.2.3 EVs as biomarkers

A biomarker is any measurable characteristic that reports physiological and/or pathological processes and responses (100). A diagnostic biomarker reports medical conditions, whilst a monitoring biomarker is used in monitoring the condition status (100). Prognostic biomarkers estimate likelihood of disease progression or recurrence, predictive biomarkers estimate response to treatment, and a response biomarker measure change following exposure or treatment (100, 101).

Cells secrete EVs under normal conditions, but secretion can increase as a response to cellular stress and pathological conditions (43). Furthermore, the composition of EV cargo has been shown to specifically alter during diseases (102-104). This, in combination with their availability through a range of biofluids including blood, cerebrospinal fluid, synovial fluid, lymph fluid, bile, nasal and bronchial lavage fluid, urine, feces, seminal fluid, breast milk and amniotic fluid (44, 105), makes EVs a promising source of biomarkers (103).

A study of urine from 21 pre-radical prostatectomy patients, and resulting tissue, found urinary EVs to carry prostate cancer gene RNAs (106). The overall accuracy of detection in EVs versus tissue was 81% (106). Furthermore, both urinary and plasma EVs have been suggested as potential non-invasive carriers of diagnostic biomarkers for several kidney diseases (107, 108). A study of protein expression in neuron derived EVs in blood of 57 Alzheimer's disease patient found expression of specific Alzheimer's pathogenic proteins to be significantly increased in EVs from patients compared to controls (109). Additionally, this approach could identify preclinical cases (109). Furthermore, miRNA expression in cerebrospinal fluid EVs has been able to diagnose Parkinson disease patients both compared to healthy controls and Alzheimer's disease controls (110).

1.2.4 Challenges in EV research

The EV research field has grown exponentially in the past couple of decades, without real standardization for EV nomenclature, -methods, or -source. As of today, there is no standard technique to isolate EVs from the source material. The isolation technique, often referred to as separation or enrichment of EVs, should be selected according to the research question as the different techniques vary in EV recovery and purity of the EV enriched sample (46). The population and composition of the isolated EVs differs based on sample processing and enrichment method, thus this method should be described thoroughly. For instance, when studying circulatory EVs, EV samples isolated from serum which allows blood clotting will contain a higher concentration of platelet derived EVs, in comparison to plasma derived EVs where an anticoagulant is added (111). The effect that different source material, processing and isolation techniques has on the population of isolated EVs and non-EV isolates makes comparison of finding between studies difficult and complicates discovery of distinguishable EV subtype markers (43, 46, 112).

A survey among ISEV members from 2019 revealed that the most used EV isolation methods, in declining order, were ultracentrifugation, size exclusion chromatography, a combination of methods, density gradient, ultrafiltration, precipitation methods and affinity capture, with more (113). Ultracentrifugation was the first method used to isolate EVs and relies on sedimentation by size and density to enrich for EVs (114). The EV source material, e.g., a biofluid or cell culture media, is first centrifuged at low speed to pellet cells and debris (114). In an iterative process with increasing centrifugal force and duration, the supernatant is then collected and recentrifuged to further specify which particles that are pelleted (114). Density gradient ultracentrifugation is a high specificity, low recovery adaption of ultracentrifugation where particles are further divided by size and density through centrifugation in a tube with a gradient density medium (46, 115, 116). The gradient is typically achieved through layering medium with different concentrations of iodixanol or sucrose (46, 115). The content of the tube is then fractionated, thus EVs of size and density of interest may be studied (115).

Furthermore, size exclusion chromatography separates particles by size. The material passes through a column with cavernous beads that disturb smaller particles, thus larger particles eluate first, and the eluate is collected in fractions (117). Ultrafiltration simply relies on membrane filtration to increase concentration of EVs and remove smaller contaminants (57). Several EV isolation kits depend on precipitation, where a volume-exclusive polymer binds

the water molecules of the material, causing less soluble elements such as the EVs to precipitate (118). Furthermore, affinity-based capture utilizes antibodies to enrich for EVs expressing one or several markers of interest to immobilize EVs on beads, plates or other media (118).

At the current stage of EV research, a wide variety of methods are in use. Notably, the methods differ in their ability to recover EVs, the specificity of the enriched EV population and presence of non-EV components in the isolate (46).

1.3 Prior studies on EVs in ME/CFS

Some exploratory studies on EVs in ME/CFS have already been conducted, of which several have an aim of searching for potential biomarkers (119-125).

In 2018, Castro-Marrero and colleagues were the first to demonstrate that the concentration of circulatory EVs was elevated in ME/CFS patients compared to healthy controls (HCs) (119). They isolated EVs using precipitation of serum from 10 patients diagnosed using the 1994 CDC/Fukuda definition and 5 HCs. In addition, they observed a difference in the EV size distribution, where EVs isolated from ME/CFS patient were on average smaller (range 103-183 nm) than those from controls (range 140-271 nm) (119).

Two years later, Almenar-Peréz et al. published their analysis of miRNA profiles from precipitation isolated plasma derived EVs and peripheral blood mononuclear cells from 15 severe ME/CFS patients diagnosed using CDC/Fukuda or CCC, and 15 HCs (120). They too observed smaller EV size and higher EV concentration in ME/CFS. Furthermore, they found 10 differentially expressed EV associated miRNAs in ME/CFS compared to HCs (120). When analyzing gene products potentially targeted by these miRNAs, they found neuronal and endocrine system pathways to be possible targets. They suggest hsa-miR-4454 & hsa-miR-7975 as top potential EV miRNA biomarker candidates (120). Recently, González-Cebrián et al. used the same dataset including blood analyte variables, miRNAs profiles of both peripheral blood mononuclear cells and EVs, EV physical features and patient information (125). They added Raman spectroscopy profiling of EVs from the same plasma samples to the dataset and fit several partial least squares-discrimination analysis models for classification of ME/CFS and developed a model using 32 parameters, of which EV physical

features (not including concentration) were important, that successfully differentiated severe ME/CFS cases from HCs (125).

Eguchi et. al. were the first to analyze ME/CFS EV associated proteins using nano liquid chromatography tandem-mass spectrometry (121). They also observed an increased concentration of circulating EVs in two groups of ~30 patients each, diagnosed with the CDC/Fukuda criteria, compared to HCs (121). Analyzing EV associated proteins, they first compared samples from three ME/CFS patients with HCs, and then four ME/CFS patients with four idiopathic chronic fatigue- and four depression patients. In both independent experiments actin network proteins were highly expressed in the ME/CFS EVs in comparison to the other groups and were suggested as potential ME/CFS biomarkers (121).

Cytokine profiling of plasma derived EVs has been carried out by Giloteaux et. al. using precipitation isolated EVs from 19 patients and 19 matched HCs (122). They observed higher EV concentration only of EVs with diameter below 130 nm (122). The cytokine profiling could not distinguish patients and HC after correction, but cytokine-cytokine interaction analysis revealed different cytokine correlation patterns in ME/CFS (122).

Recently, Bonilla et. al. compared plasma derived EVs from 20 HCs to 10 mild cases and 10 severe cases of ME/CFS diagnosed using the CDC/Fukuda criteria (123). They stained EVs in plasma with markers for EV surface molecules that identifies the EVs' cell type of origin (123). They found a correlation between severe ME/CFS and level of B-cell- and platelet originating EVs, which did not withstand correction (123). Contrary to previous studies, elevated levels of EVs in patients was not replicated (123).

Tsilioni, Natelson and Theoharides have detected EV associated mitochondrial DNA from ME/CFS patients and HCs (124). Affinity isolated serum-derived EV samples from patients were investigated both before and after exercise. They found the level of mitochondrial DNA in EVs to be significantly increased following exercise (124). They then exposed cultured human microglia cells to pooled EV samples from the different groups. As a result, they observed an increased concentration of the pro-inflammatory cytokine interleukin 1β in the medium of those exposed to ME/CFS post-exercise EVs (124). They hypothesize that increased EV associated mitochondrial DNA trigger local autoinflammatory responses in the hypothalamus (124).

Several of these studies had limitations regarding cohort sizes, diagnostic- and exclusion criteria. They use different EV sources, and techniques for isolation, EV quantification, and -size detection that makes them difficult to compare. Yet, most of them suggest a potential implication of EVs in ME/CFS, and further highlight EVs as potential sources of biomarkers for the disease, however this needs further investigation. Previously, EVs have been implicated in immune- and central nervous system disorders with symptom overlap to ME/CFS (99, 126, 127). The minimally invasive availability of EVs through biofluids, and their implication in diseases with shared symptomology fortify the need for further investigation of EVs in ME/CFS. Considering the role of EVs in transferring functional cargo between cells, and how EV secretion is affected by cell state, ME/CFS EV research poses the potential for insight into ME/CFS pathogenesis and discovery of biomarkers. The extensiveness and range of different diagnostic criteria used today contributes to low diagnosis rates and observed heterogeneity of patients respectively. Thus, discovery of a minimally invasive diagnostic biomarker for ME/CFS would greatly benefit patients, clinicians and researchers.

2. Aim of study

With the underlying hypothesis that ME/CFS is an immune-mediated disease, the overall aim of this thesis was to explore EVs in ME/CFS and their potential as biomarkers. Another goal was to optimize EV research methodology transferable to research projects on other diseases.

Research objectives:

- Assess the enrichment of EVs from blood plasma by size exclusion chromatography, through EV characterization by western blotting, transmission electron microscopy and analysis of data from nanoparticle tracking analysis.
- Investigate EV characteristics including concentration, size and morphology between ME/CFS patients and healthy controls.
- Initiate analysis of EV proteomics data for future biomarker studies in ME/CFS.

3. Materials and methods

This master project is a continuation of work performed at OUS. Prior to this project, the Genetics of Autoimmunity research group at the Department of Medical Genetics at OUS received and isolated EVs from plasma samples from 20 ME/CFS patients and 20 HCs. These EV enriched samples were used in nanoparticle tracking analysis and label free mass spectrometry. The resulting data were later provided to the master project for analysis which is presented in this thesis. Furthermore, EVs were re-isolated from the same patients and controls during the project, using different aliquots of the same plasma samples.

3.1 Clinical samples

For this project, blood plasma samples from ME/CFS patients diagnosed according to the CCC (10) (n= 20) and healthy controls (n=20), were used as a source of EVs. Plasma and clinical data had previously been collected between 2013 and 2019 by the CFS/ME center. The CFS/ME center's biobank possesses plasma samples from patients diagnosed or treated at the center, and plasma from healthy controls collected from first time donors to the blood bank at OUS (128). Records of sex, age, body mass index (BMI) and cardiovascular disease at time of inclusion was provided for both patients and controls, however smoking status was not. If an ME/CFS patient was a bedpost patient or presented atypical ME/CFS (e.g. non-infectious disease onset), this was stated, but time since disease onset or severity was not provided.

3.1.1 Sample collection and plasma processing

The CFS/ME center prepared the plasma samples as follows. Blood was collected in 10 ml BD Vacutainer® PlusPlastic K_2 EDTA tubes and centrifuged within 30 minutes after collection at 1800 *g* for 15 minutes at room temperature. The top portion of the plasma was transferred to microtubes, avoiding the last 0.5 cm before the buffy coat. Within 10 minutes after the initial centrifugation, the plasma was further centrifuged at 15000 *g* for 15 minutes at 4 °C. The plasma, avoiding the pellet, was aliquoted, frozen, and stored at -80°C.

3.2 EV isolation by size exclusion chromatography

Size exclusion chromatography (SEC) separates particles based on size and was used to enrich for EVs from plasma (see Figure 2). During SEC, plasma passes through a column containing porous beads. Larger particles will not be disturbed and thus elute faster than smaller particles. The eluate from the column is collected into different fractions (F), and EV-enriched fractions are pooled. This does not yield a pure EV isolate but rather an EV enriched sample, a sample of higher concentration of EVs relative to other plasma components.

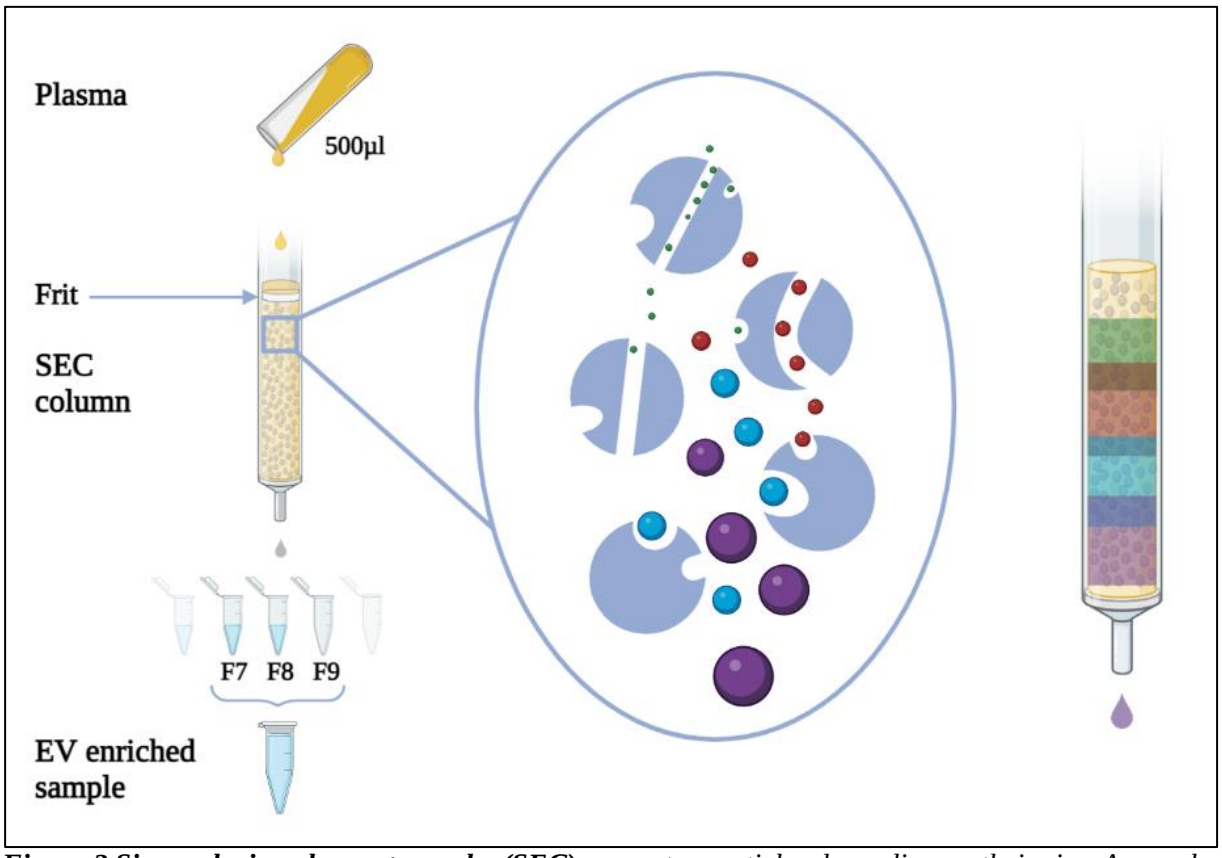

Figure 2 Size exclusion chromatography (SEC) *separates particles depending on their size. A sample is passed through a size exclusion column. The column contains cavernous beads that extend the travel of smaller particles, thus causing them to eluate later than larger particles. SEC is used to isolate EVs from plasma, by pooling EV enriched fractions (F7-F9). Figure created in Biorender.com.*

SEC was performed by loading 500 µl plasma into an qEVoriginal 70 nm legacy column (SP1, Izon Science, Christchurch, New Zealand) on the Automatic Fraction Collector V1 (AFC) (Izon Science) following the instructions on the display of the AFC, and the AFC(V1) user manual (129), with some deviations.

A room temperature column was mounted on the AFC. The AFC scale was calibrated with the included 10 g weight at the beginning of each day and repeated at a minimum between every 10 runs. The collection schedule was set accordingly: Void volume: 2.7 ml, Fraction volume: 0.5 ml, No. of fractions: 5. The new column was flushed with 15 ml freshly 0.2 µm filtered Dulbecco's phosphate-buffer saline (DPBS) (1x) no magnesium, no calcium (14190-094, Gibco, Billings, MT, USA). Immediately as the DPBS had gone below the loading frit (see Figure 2), flushing was halted and 500 µl plasma thawed on ice was applied to the column. Directly after the sample had gone below the frit, 7 ml filtered DPBS was added to the column. The first five fractions, the void volume, were not collected while the last five fractions were collected in labelled 2ml Eppendorf tubes in the carousel of the AFC. Fractions 6 and 10, collected in tubes in position 1 and 5 of the carousel, were discarded. Eppendorf Protein LoBind® tubes were used in position 2, 3 and 4, to collect EV enriched fractions 7, 8 and 9 that were pooled to yield 1500 µl EV enriched sample, as recommended by the manufacturer. Between each run, the column was flushed with 25 ml filtered DPBS before the next plasma sample was applied. Each column was used for a maximum of 5 plasma samples, and the order of samples applied to the columns were randomized.

SEC was performed with plasma aliquots from the same 20 patients and 20 controls whose EV samples were used in nanoparticle tracking analysis and mass spectrometry. This was done to replace the used samples and will be included in future proteomics analyses. To yield EV enriched samples for use in optimization of western blotting and transmission electron microscopy, SEC was repeated with test plasma. For the final experiments, SEC was performed to create representative EV pools enriched from plasma pools from each cohort. Five patients and five controls were randomly selected using the "select()" function in base R (version 4.2.0). 100 µl plasma from each of them were pooled to yield one representative ME/CFS plasma pool and one representative HC plasma pool from which EVs were enriched resulting in one ME/CFS EV pool and one HC EV pool.

3.2.1 Ultrafiltration

Ultrafiltration was used to increase the concentration of EVs in an aliquot of the ME/CFS EV pool (n=5) and the HC EV pool (n=5), prior to western blot analysis and transmission electron microscopy. In addition, EV enriched samples from test plasma were ultrafiltrate prior to use in optimization of western blotting and transmission electron microscopy.

Ultrafiltration was performed by applying a 1200 µl aliquot from each EV pool into the filter device of an assembled Amicon® Ultra-2 centrifugal filter unit (UFC200324, Merck Millipore, Burlington, MA, USA). Centrifugal filters with EV enriched samples were centrifuged in an Eppendorf 518 R benchtop centrifuge at 2000 *g* at 4℃ until 4x concentrated to 300 µl. The filtrate tube with filtrate was discarded. The remaining filter unit was flipped and placed back into the centrifuge, with the concentration collection tube down, and was centrifuged at 1000 *g* for 2 minutes at 4℃. The concentrate was collected to yield 4x concentrated EV pools from ME/CFS and HC. Samples for TEM were kept on ice or at 4℃ and were delivered fresh for analysis the day of isolation and ultrafiltration, while samples used in western blot analysis were lysed and stored at -20℃.

3.2.2 Software update

Between the EV isolation previously performed by researchers at OUS and the re-isolation performed during the master project, the AFC(V1) underwent a software update: AFC(V1) update 2.6.2 (130). This altered the possible void volumes in the collection schedule, which initially was 2.8 ml and was 2.7 ml after the update. In future proteomics analyses that utilize EV samples from both rounds of isolation, this will be investigated as a possible batch effect.

3.3 Western blotting

Western blotting is a semi-quantitative technique used to detect the presence of specific proteins in a complex mixture using antibodies (131). Proteins are separated in a gel according to molecular weight before transfer to a membrane. Immobilized proteins on the membrane are then incubated with a primary antibody specific to the protein of interest, followed by incubation with a secondary antibody that forms a complex with the primary antibody (132). In this project, the secondary antibody of choice was conjugated to horseradish peroxidase (HRP) enzyme. When exposed to a chemiluminescent substrate containing peroxide and luminol the HRP oxidizes luminol which emits a light signal captured by an imaging instrument, thus visualizing the protein of interest (132).

To validate presence of EVs in the EV enriched samples, antibodies recognizing established EV markers were used (46) (Appendix 1). Namely membrane bound tetraspanins CD9 and CD63, and the enclosed ESCRT accessory protein tumor susceptibility gene 101 (TSG101). Detection of the plasma abundant protein albumin was also performed. All antibodies used

throughout this thesis, including the optimization, are listed in **Error! Reference source not found.**Appendix 1.

3.3.1 Lysis of EV enriched samples

Prior to western blotting, freshly isolated EV enriched samples were lysed to expose enclosed proteins. RIPA lysis buffer 10x (20-188, Merck Millipore, Darmstadt, Germany) was mixed with Halt™ Protease and Phosphatase Inhibitor Cocktail (100X) (78440, Thermo Fisher Scientific™, Waltham, MA, USA), to avoid protein degradation, and added to each sample. Samples were then mixed by vortexing for 30 seconds and incubated on ice for at least 15 minutes. Lysed samples were aliquoted and stored at -20℃.

3.3.2 Gel electrophoresis and membrane blotting

The optimized western blotting procedure for detection of each target protein varied depending on the choice of primary antibody, sample buffer, blocking reagent and dilution of antibodies (Table 1).

Table 1: Parameters used in final western blots *for detection of CD9, CD63, TSG101 and Albumin from lysed plasma extracellular vesicle samples.*

Target protein	**Sample buffer**	**Primary antibody (clone) (catalog number, supplier)**	**Primary antibody dilution (concentration)**	**Blocking reagent**	**Secondary antibody dilution (concentration)**
CD9	4x Laemmli (1610747, Bio-Rad)	CD9 Monoclonal Antibody (Ts9) (10626D, Invitrogen)	1:500 (1µg/ml)	5% bovine serum albumin	1:2000 (1µg/ml)
CD63	4x Laemmli (1610747, Bio-Rad)	CD63 Monoclonal Antibody (Ts63) (10628D, Invitrogen)	1:500 (1µg/ml)	5% bovine serum albumin	1:2000 (1µg/ml)
TSG101	3x sample buffer with DTT	TSG101 Monoclonal Antibody	1:1000 (1.74µg/ml)	5% skim milk	1:1000 (2µg/ml)

		(4A10) (MA1-23296, Invitrogen)			
Albumin	3x sample buffer with DTT	ALB (F-10) (sc-271605, Santa Cruz Biotechnology)	1:1000 (0.2µg/ml)	5% skim milk	1:1000 (2µg/ml)

30 µl aliquots of lysed EV enriched sample were thawed on ice before mixing with appropriate room temperature sample buffer. For samples used in detection of CD9 and CD63, samples were mixed with non-reducing 4x Laemmli sample buffer (1610747, Bio-Rad). Samples for detection of TSG101 and albumin were mixed with premade 3x sample buffer with reducing agent dithiothreitol (DTT) (Formulation: 1.5 ml 1M Tris-HCl (pH 6.8), 6.0 ml 10% SDS, 1.0 ml 2% bromophenol blue, 1.5 ml 99% glycerol and 1 ml 1M DTT). Samples with sample buffer were boiled for 5 minutes at 97 ℃ on a heat block, spun and placed back on ice. 40 µl sample or 10 µl ladder, Precision Plus Protein Dual Color Standards (1610374, Bio-Rad), was loaded into the wells of 4–20% Mini-PROTEAN® TGX™ Precast Protein Gels, 10-well, 50 µl (4561094, Bio-Rad). The electrophoresis chamber was filled with 1x Tris/Glycin/SDS Buffer (1610732, Bio-Rad) and gel electrophoresis was run at 110 V for 95-98 minutes.

Per gel, four sponges, four pieces of thin blot paper (1620118, Bio-Rad) and one piece of 0.2 µm nitrocellulose membrane (1620112, Bio-Rad) were soaked in transfer buffer (1x Tris/Glycine Buffer (1610734, Bio-Rad) with 20% methanol). A transfer sandwich was assembled by layering two sponges, two blot papers, gel, membrane, two blot papers and sponges in the given order, avoiding air bubbles. The sandwich was placed into a chamber, oriented with the membrane between the gel and the positive anode (See Figure 3). The chamber was filled with transfer buffer. An ice block and magnet were added, and proteins were transferred from gel to membrane at 100 V for 20 minutes with stirring by magnet. The protein transfer was investigated by incubating the membranes with Ponceau S solution (P7170, Sigma-Aldrich, Darmstadt, Germany) for 5 minutes with shaking at room temperature. Ponceau S solution was removed by washing with 1x Tris Buffered Saline (1706435, Bio-Rad) with 0.1% Tween 20 (P1379, Sigma-aldrich) (TBS-T) with shaking, replacing the TBS-T until no red color was left.

Membranes used for CD9 and CD63 detection were blocked with 5% bovine serum albumin (BSA) (A7906, Sigma-Aldrich) in TBS-T for 1 hour with shaking at room temperature. Membranes for TSG101 and albumin detection were blocked with 5% skimmed milk (70166, Sigma-Aldrich) in TBS-T for 1 hour with shaking at room temperature. After blocking, membranes were washed with TBS-T swiftly, as not to disturb the blocking, before transfer to 50 ml falcon tubes with 10 ml appropriate primary antibody diluted in TBS-T with 0.02% sodium azide. Membranes were incubated with primary antibody solution on roller overnight at 4°C.

The following day, membranes were washed for 3x10 minutes in TBS-T with stirring before incubation on roller at room temperature for 1 hour with HRP-conjugated secondary antibody (Anti-mouse IgG, HRP-linked Antibody, 7076, Cell Signaling Technology, Danvers, MA, USA) diluted in 5% skimmed milk in TBS-T. Secondary antibody was diluted 1:2000 for incubation with CD9- and CD63-, and 1:1000 for TSG101- and albumin membranes. Membranes were washed 3x 10 minutes with TBS-T.

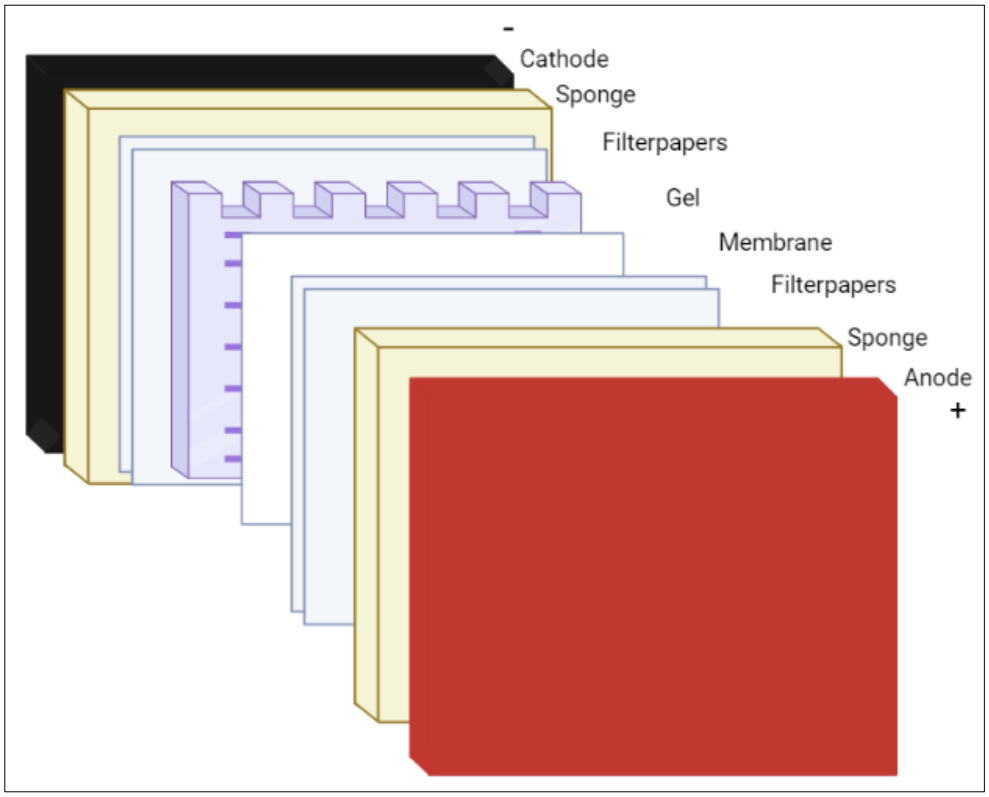

Figure 3: Western blot transfer sandwich *assembled for transfer of proteins seperated in gel to membrane. Sponges, filter paper, gel and membrane is assembled into a sandwich and is submerged in transfer buffer. The sandwich is subjected to current where the proteins move towards the positive anode, thus the membrane must be placed between the gel and the anode. Proteins are transfered from*

gel to memabrane to immobilize the proteins and make them easier to handle since the memebrane is more robust than gel. The figure was created with biorender.com.

3.3.3 Western blot imaging

Prior to imaging, membranes in TBS-T were cut with a clean scalpel to separate the concentrated- and not concentrated EV protein samples, to avoid overshadowing of the signal from the not concentrated samples.

For each piece of membrane, equal amounts (500 -1000 µl depending on membrane size) of reagent A and B of ECL™ Prime Western Blotting Detection Reagent (RPN2232, Cytiva, Marlborough, MA, USA) were mixed to generate a detection reagent. The membrane was moved to a sheet of plastic, and the detection reagent was pipetted onto the membrane. The membrane was left on the bench for 1 minute to develop, before transfer to a black tray in the imaging machine, ImageQuant LAS 4000 (GE healthcare, Chicago, IL, USA).

The imaging machine had already been cooled to -25°C, and in the ImageQuant LAS 4000 software (version 1.2) settings had been set accordingly. Exposure type: Precision, Exposure time: Manual, Sensitivity/Resolution: Standard, Add digitalization image: ON, Method: Chemiluminescence, Tray position: 1. Starting exposure time was 5 seconds, increasing to 15, 30, 60 and 120 or 240 seconds if no bands appeared at 60 seconds. Each image was saved as a 16-bit.tif file. A multiplex image of each blot was created in ImageQuant TL software (version 8.1.0.0).

3.4 Transmission electron microscopy (TEM)

TEM is an imaging technique commonly used to directly visualize nanoparticles and their morphology. A fixed biological sample is exposed to a beam of electrons in vacuum. The electrons either scatter as they interact with the atoms of the sample or pass through and hit a detector. This results in a high-resolution image, where darkness represents density in the sample. In negative stain TEM the sample is stained with a heavy metal (e.g. through using uranyl acetate), resulting in a dark outline of the particle structure on the final image (133). Immuno-TEM uses gold conjugated antibodies to a protein of interest to further identify and characterize the observed structures (134). In TEM for characterization of EVs, immunogold labeling against a surface EV marker, e.g. CD63, is commonly used (134).

3.4.1 Negative stain- and immuno-TEM

Negative stain- and immuno-TEM was conducted as follows by the Advanced Electron Microscopy Core Facility at the Institute for Cancer Research, OUS. Five µl representative EV enriched sample was applied to formvar/carbon grids and incubated for 10 minutes at room temperature. EVs were fixed in 4% formaldehyde and 0.1% glutaraldehyde for 15 minutes, followed by 2x 1 minute washing with PBS. For immunogold labelling of CD63-positive EVs, grids were blocked by incubation with 0.5% BSA in PBS for 10 minutes followed by incubation with mouse CD63 primary antibody (H5C6, Developmental Studies Hybridoma Bank, University of Iowa, Iowa city, IA, USA), diluted 1:50 in 0.5% BSA in PBS, for 20 minutes. After 5x 5minutes washing with PBS, the grids were incubated for 20 minutes with rabbit anti-mouse secondary antibody (315-005-044, Jackson Immunoresearch, Camebridge, UK) diluted 1:1500 in 0.5% BSA in PBS, and then washed with PBS for an additional 5x 5 minutes. Finally, grids were incubated for 15 minutes with 10 nm protein A-gold, diluted 1:50 in 0.5% BSA in PBS, and then first washed 5x 1 minute with PBS and 5 x 1 minutes with water. For negative staining of EVs, blocking and incubation with antibodies and A-gold was not preformed. Particles were stained and embedded in 0.4% uranyl acetate and 1.8% methyl cellulose for 10 minutes at 4℃ and then left to dry for 20 minutes at room temperature. The samples were viewed with a JEOL JEM-1230 transmission electron microscope operated at 80 kV and photographed with a Morada digital camera. This was repeated for the concentrated- and not concentrated ME/CFS and HC EV pools.

3.5 Nanoparticle tracking analysis (NTA)

NTA was used to quantify EVs and determine their mean- and mode size, in the EV enriched samples of all patients and controls. NTA utilizes light scattering to analyze nanoparticles in suspension. During NTA a laser illuminate particles, and a video camera captures the scattered light. Using the video, the NTA software then identifies each individual particle and analyzes their Brownian motion. Smaller particles have higher velocity Brownian motion. The software counts each particle which yields particle concentration and uses their velocity to calculate their size by applying it in the Stokes-Einstein equation (135).

NTA was performed by the Department of Medical Biochemistry, OUS, using NanoSight NS500 (Malvern Instruments Ltd, Malvern, UK), with Software version 3.40 (Malvern

Instruments Ltd). An accessory NanoSight Syringe Pump (Malvern Instruments Ltd.) was used to ensure even flow of particles into the instrument. The NTA instrument was calibrated by running with 100 nm polystyrene beads. A 10 µl freshly isolated aliquot of each SEC EV enriched sample was diluted 1:100 in 0.02 µm filtered PBS. Next, 0.7 – 0.9 ml diluted sample in a syringe was attached to the syringe pump. Pumping began with an infusion rate of 1000, then rapidly halving the rate until 20. The particles were visualized with camera level 14, and recording was initiated. When finished, detection level was set to 4 and the software quantified EVs and calculated their size. The pump and instrument were flushed with water between each run. This was repeated for all 20 patient- and 20 HC EV samples. Each sample was analyzed in triplicate, and the results were averaged.

3.6 Identification of EV associated proteins by mass spectrometry

Mass spectrometry is a technique used for identification and quantitation of different chemical compounds and is commonly used in proteomic profiling of biological samples. The analytes are ionized, separated based on mass-to-charge ratio and detected. Several mass spectrometry methods exist. In this project, protein content of EV samples was detected with liquid chromatography tandem mass spectrometry (LC-MS/MS). During LC-MS/MS with electron spray ionization, liquid sample containing analyte is passed through a capillary with an electron field and charges the sample. Charged drops of sample are sprayed from the capillary into vacuum and is subjected to a flow of heated nitrogen gas (136). This dries the electrically charged drops which burst into smaller droplets. Continuous drying and bursting of charged droplets to smaller droplets results in emission of ionized analytes from the droplets (136, 137). These ions are then directed into the first mass filter, a quadrupole of rods which is connected to radiofrequency and direct current which only allow analytes of a specific mass-to-charge ratio to pass through to the collision cell (136, 137). There, the selected analytes collide with molecules of a collision gas causing fragmentation. The product ions are directed into a mass analyzed. Again, only a specific ion product passes through the second quadrupole, while others will fall out. Thus, only a specific fragment of a specific analyte reaches the final time of flight detector following the second quadrupole (137). The frequencies can be altered quickly to allow detection and quantification of several analytes.

The LC-MS/MS was performed by the Proteomics Core Facility at OUS (138). For each EV enriched sample, a 120 µl aliquot was lysed and digested by mixing with 11 µl 1% ProteaseMax Surfactant in 50 mM NH_4HCO_3. Samples were vortexed for 10 seconds and incubated at 95℃ for 20 minutes. Protein concentrations were measured by bicinchoninic acid assay and samples were frozen overnight. The following day, 2 µl 0.5 mM DTT was added to the samples before incubation at 56℃ at 30 minutes. Then, 3.2 µl 550 mM indoleacetic acid was added to the samples which were incubated at room temperature for 1 hour. Samples were then further diluted with 240 µl 50 mM NH_4HCO_3 to reach ProteaseMax concentration of 0.033%. Finally, 0.5 µg trypsin (Promega, Madison, WI, USA) was added before incubation at 37℃ overnight.

An equal volume of each sample was purified and concentrated using C18 tips. Samples were analyzed with nanoElute (Bruker, Billerica, MA, USA) liquid chromatography system coupled to the timsTOF flex (Bruker) spectrometer, using a 1 hour separation gradient.

In MaxQuant (version 2.0.3.0), resulting raw files were analyzed against the Uniport human database (from 2020) for protein identification, and label-free quantification. Parameters were set as follows. Fixed modification: Carbamidomethyl, Variable modifications: N-acetylation and methionine oxidation, First search error: 22 ppm, Main search error: 6 ppm. The option of trypsin without proline restriction enzyme was chosen. For protein identification setting were set as: Minimal unique peptides: 1, False discovery rate allowed: 0.01. False discovery rate was assigned by generation of reversed sequences. Reversed sequences and known contaminants were removed.

3.7 Statistical analyses and quality control

All software used throughout the project are listed in Appendix 2.

3.7.1 Analysis of patient and control demographics.

To assess if patients and controls were matched according to sex, age and possibly BMI the data was analyzed in R version 4.2. Distribution normality was assessed with histograms using “ggplot()” with “geom_histogram()” form R-package ggplot2 (139), quantile-quantile plots created with the “ggqqplot()” function from R-package “ggpubr”(140), and Shapiro-Wilk normality tests performed using the “shapiro.test()” function in base-R. For data that

was normally distributed in both cohorts, f-test assessment of equal variance was performed with the “var.test()” function. Normalized sets of data with equal variances were analyzed with two sample t-test using “t.test()” specifying “var.equal=TRUE”. Non-normally distributed data was analyzed with nonparametric Mann-Whitney U-tests, also known as the Wilcoxon rank sum test, using the “wilcox.test()” function in base-R.

3.7.2 NTA data analysis

NTA data on EV concentration, mean- and mode EV size in each cohort was assessed and analyzed as described in section 3.7.1 above. The resulting histograms and qq-plots of NTA data are presented in Appendix 3, supplementary figure 1-6. Normally distributed pairs of data were analyzed with two-sample t-test, and non-normally distributed data with Mann-Whitney U tests. From the R-package “ggplot2” (139), “ggplot()” with “geom_boxplot()” was utilized to illustrate the distribution of mean EV concentration and mean- and mode EV size within the two cohorts as boxplots.

3.7.3 Analysis of EV associated proteins using FunRich

The resulting MaxQant analyzed mass spectrometry data of detected proteins and repsecitve intensity from all EV enriched samples from both the ME/CFS and HC cohort were treated and analyzed with Excel (version 2211), R (version 4.2) and FunRich (version 3.1.3). Peptides marked as possible contaminants were removed from the dataset. Using normalized label-free quantitation (LFQ) intensity, lists of detected peptides in each cohort were made. The associated gene names of all detected proteins were inserted into FunRich since gene names were required as input to compare with Vesiclepedia. FunRich was used specifically to allow analysis with data from Vesiclepedia, an EV database of previously detected EV proteins, RNA molecules and lipids in EVs (141). In FunRich, Vesiclepedia data was loaded with settings species: *Homo sapiens,* content types: proteins. A Venn diagram was created to evaluate the overlap of detected peptides with Vesiclepedia. With protein ID as input, a Venn diagram of detected proteins within the two cohorts was created. Exclusively detected proteins within each cohort were further studied in FunRich and Excel.

Due to discovery of batch effect caused by clogging of the mass spectrometer, differential expression analysis of EV associated proteins was postponed and not performed as a part of this thesis as initially planned.

4. Results

4.1 Demographics of patients and controls

All patients and controls were female and were matched for age as no significant differences was observed (p=0.9) (Table 2). However, the cohorts were not fully matched for BMI (p = 0.5), as BMI was higher in controls than patients.

Table 2: Age, body mass index (BMI) and sex of ME/CFS patients and HCs *at time of blood sample collection. For one patient, BMI was not recorded.*

	ME/CFS patients (n = 20)	**HCs (n = 20)**	**p-value**
Age, mean ± SD	41.3 ± 10.9	40.9 ± 10.6	0.9
BMI, mean ± SD	23.8 ± 4.6	25.7 ± 3.7	0.05
Females (in %)	20 (100)	20 (100)	1

4.2 Western blot optimization

Optimization of the western blot protocol was performed in several iterations to ensure we could detect minimum three EV markers in the EV enriched samples of which at least one was a surface marker, and one was enclosed in the EVs. The parameters of optimization included dilution of both primary and secondary antibody, choice of blocking reagent and sample buffer with or without reducing agent DTT. All optimization experiments used lysed, concentrated EV samples enriched from test plasma.

For initial detection of EV surface marker CD9, a primary antibody from Santa Cruz Biotechnology (sc-13118) yielded a blot with several unspecific bands and low detection of CD9 at expected molecular weight of 24 kDa (Figure 4, A), and was thus eliminated. The same procedure with a CD9 antibody from Invitrogen (10626D, Waltham, MA, USA) (Table 3, B) resulted in a black blot (Figure 4, B). We hypothesized that skimmed milk was an unsuitable blocking reagent for the primary antibody, and thus preformed the optimization set up presented in table 3 C-D.

Table 3: Optimization set up for detection of CD9. A) *Procedure for initial CD9 detection with primary antibody from Santa Cruz biotechnology.* ***B)*** *Procedure for detection of CD9 using primary antibody from Invitrogen* ***C- D)*** *pieces of the same membrane subjected to different conditions to trouble shoot and optimize conditions for use of the Invitrogen CD9 antibody.*

Blot	CD9 primary antibody supplier (catalog number)	Sample buffer (boiling conditions)	Blocking agent	CD9 antibody diluent
A	Santa Cruz Biotechnology (sc-13118)	With DTT (97°C, 5 min)	Skimmed milk	TBS-T with sodium azide
B	Invitrogen (10626D)	With DTT (97°C, 5 min)	Skimmed milk	TBS-T with sodium azide
C	Invitrogen (10626D)	Without DTT (70°C, 10 min)	Bovine serum albumin	Bovine serum albumin
D	Invitrogen (10626D)	Without DTT (97°C, 5 min)	Bovine serum albumin	TBS-T with sodium azide
E	Invitrogen (10626D)	With DTT (97°C, 5 min)	Bovine serum albumin	Bovine serum albumin

From the resulting blots of the CD9 troubleshooting procedure, BSA appeared to be a more suitable blocking reagent, and no additional reducing agent in the sample buffer was needed (Table 3 and Figure 4). The protocol for blot D was deemed the most successful in CD9 detection out of the four (Table 3 and Figure 4).

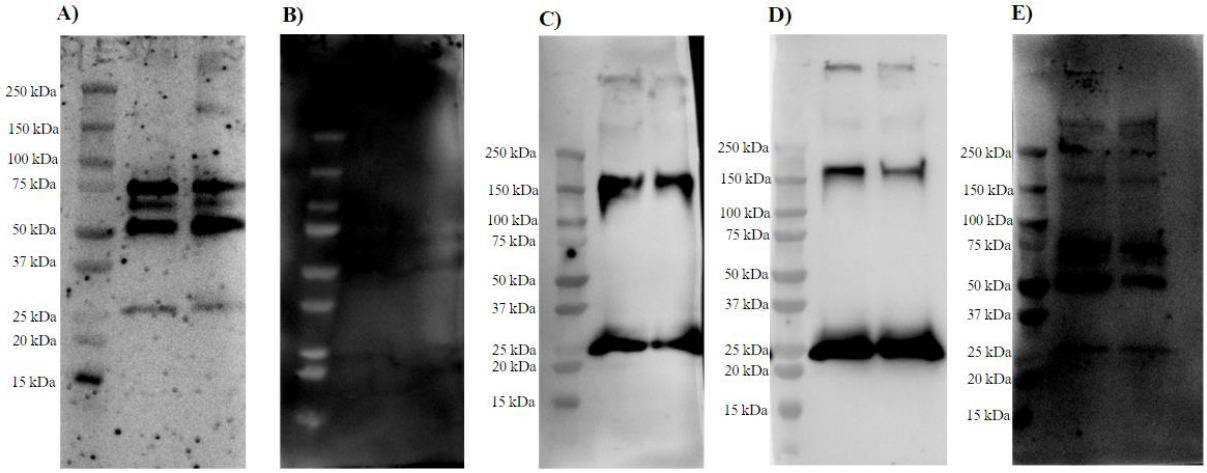

Figure 4: Western blot results of CD9 trouble shooting*. The different conditions per blot are described in table 3.*

Furthermore, western blot experiments for detection of CD63, CD81, TSG101 and albumin were tested. This resulted in detection of all aforementioned proteins, except CD81. As a result, CD81 was excluded from further experiments as detection of three EV markers was sufficient according to MISEV2018 (46).

4.3 Successful detection of CD9, CD63, TSG101, and albumin by western blotting

The final western blot experiments resulted in successful detection of the three EV markers, CD9, CD63 and TSG101, and albumin in the EV pools enriched from plasma pools of five ME/CFS patients and five HCs.

CD9 was detected in both the EV pool and concentrated EV pool, blot A and B respectively, for both ME/CFS patients and controls (Figure 5). The bands representing detection of CD9 were observed in both blots at 24 kDa outlined by a blue box. In addition, unspecific bands were present at about 150-200 kDa.

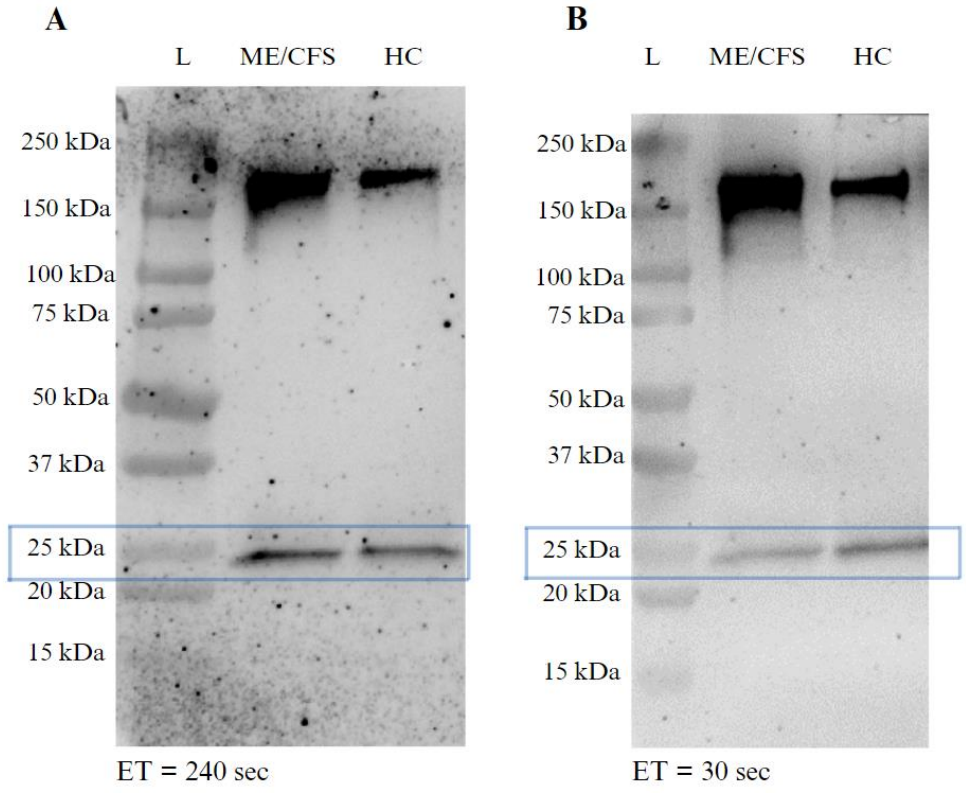

Figure 5: Western blot analysis for detection of CD9 in ME/CFS EV pool (n=5) and HC EV pool (n=5) using monoclonal mouse CD9 antibody (1 µg/ml) and anti-mouse horseradish peroxidase linked secondary antibody (1

µg/ml). **A**) Not concentrated EV pools. **B**) EV pools were 4x concentrated by ultrafiltration prior to lysis. Abbreviations: L = Ladder, ET = exposure time in seconds. Blue boxes outline expected CD9 bands.

The western blot experiments confirmed presence of CD63-positive EVs in the ME/CFS- and HC EV pools, where characteristically smeared bands representing detection of CD63 were present at about 30-60kDa marked by the blue boxes (Figure 6). Detection of CD63 in the EV pools which were not concentrated was faint (Figure 6, A).

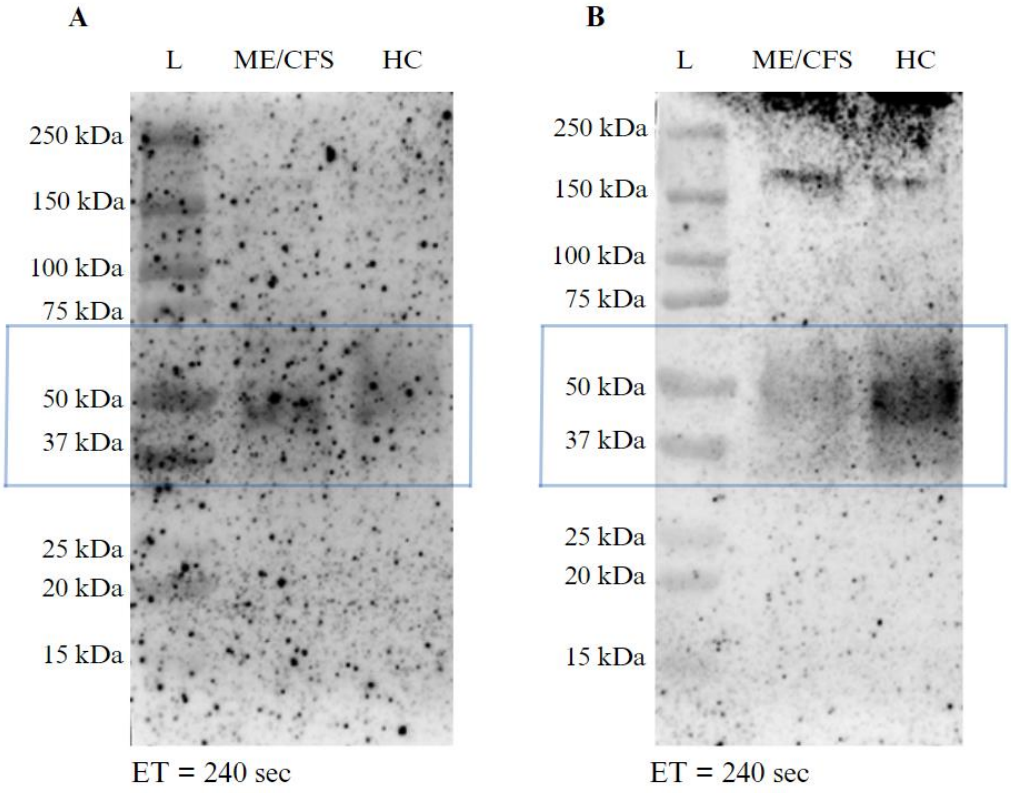

Figure 6: Western blot analysis for detection of CD63 in ME/CFS EV pool (n=5) and HC EV pool (n=5) using monoclonal mouse CD63 antibody (1 µg/ml) and anti-mouse horseradish peroxidase linked secondary antibody (1 µg/ml). **A**) Not concentrated EV pools. **B**) EV pools were 4x concentrated prior to lysis by ultrafiltration. Abbreviations: L = Ladder, ET = exposure time in seconds. Blue boxes outline expected CD63 bands.

TSG101 was detected in both the EV pool and the concentrated EV pool enriched from the ME/CFS plasma pool (n=5) and the HC plasma pool (n=5), as bands representing detection of TSG101 are present in all lanes of the blots (Figure 7). Bands representing TSG101 detection appeared in the 55-70 kDa region, marked with a blue box.

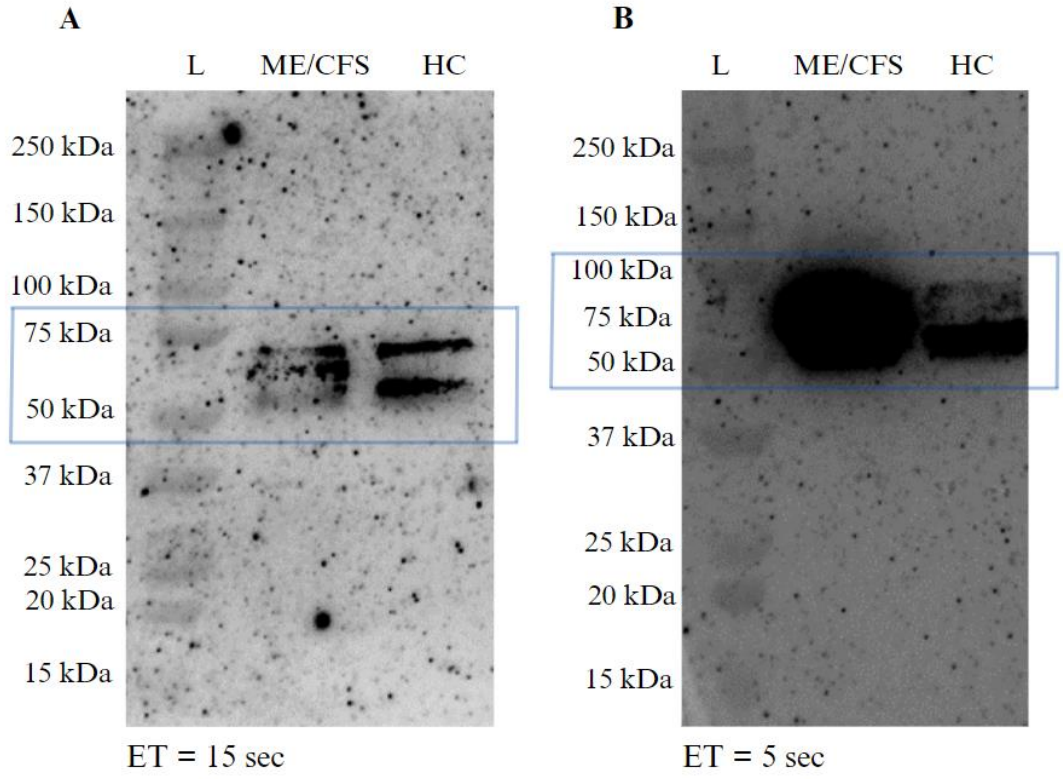

Figure 7: Western blot analysis for detection of TSG101 in ME/CFS EV pool (n=5) and HC EV pool (n=5) using monoclonal mouse TSG101 antibody (1.74 µg/ml) and anti-mouse horseradish peroxidase linked secondary antibody (2 µg/ml). **A**) Not concentrated EV pools. **B**) EV pools were 4x concentrated prior to lysis by ultrafiltration. Abbreviations: L = Ladder, ET = exposure time in seconds. Blue boxes outline TSG101 bands.

Bands representing detection of albumin are present in both lanes of both blots, thus albumin was detected in both the EV pool and concentrated EV pool enriched from the ME/CFS plasma pool (n=5) and the HC plasma pool (n=5) (Figure 8). This indicates the presence of plasma co-eluates. Albumin bands, framed by blue boxes, are present between 52-70 kDa. The difference in band thickness on blots indicates higher levels of albumin in the representative ME/CFS EV pool than the HC EV pool.

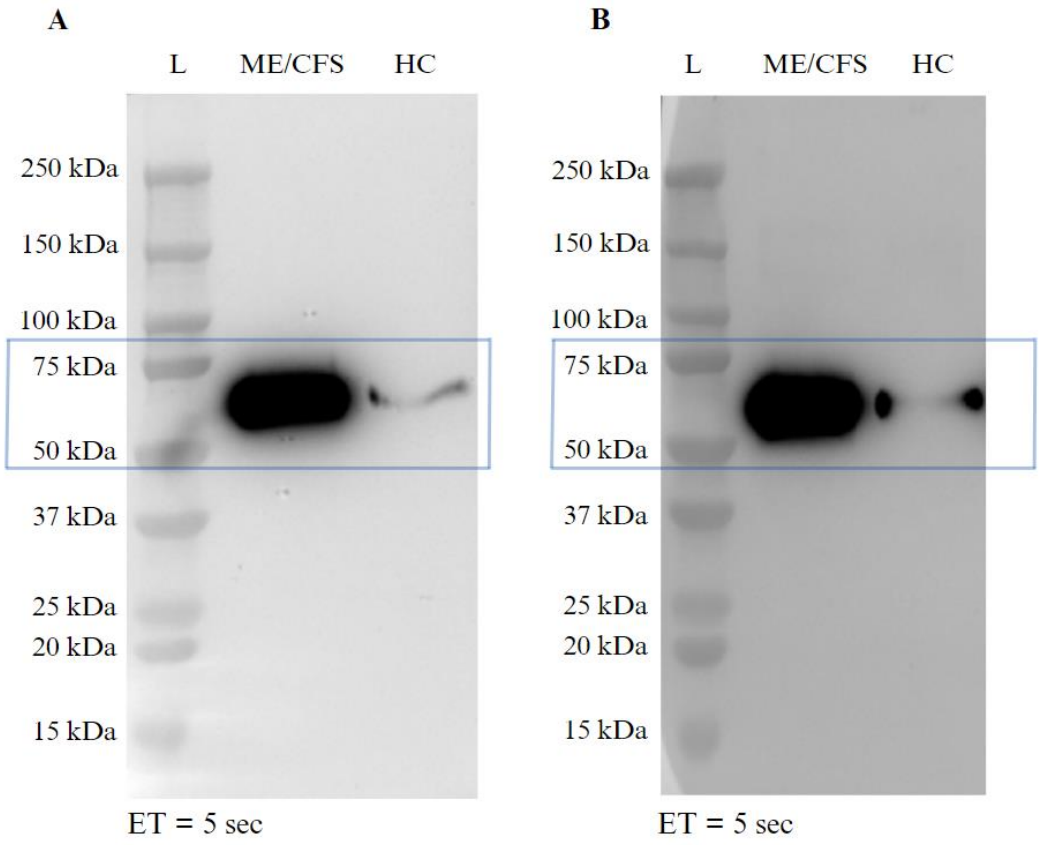

Figure 8: Western blot analysis for detection of albumin in ME/CFS EV pool (n=5) and HC EV pool (n=5) using monoclonal mouse albumin antibody (0.2 µg/ml) and anti-mouse horseradish peroxidase linked secondary antibody (2 µg/ml). **A**) Not concentrated EV pools. **B**) EV pools were 4x concentrated prior to lysis by ultrafiltration. Abbreviations: L = Ladder, ET = exposure time in seconds. Blue boxes outline expected albumin bands.

The western blot experiments detected EV markers CD9, CD63, TSG101 in the SEC enriched ME/CFS- and HC EV pools. This contributes to validation of presence of EVs in the EV enriched samples. In addition, detection of albumin indicates presence of co-eluates or contaminants.

4.4 Transmission electron microscopy confirms presence of EVs

To further validate the presence of EVs and compare ultrastructure of EVs between the two cohorts, we analyzed negative stain- and immuno-TEM micrographs of ME/CFS- and HC EV pools and concentrated EV pools. EVs were observed in the negative stain micrographs, and

the immuno-TEM further confirmed that the structures seen in fact were EVs, as immunogold labeling of EV marker CD63 allowed distinguishing from other co-eluates.

4.4.1 Negative stain-TEM

Intact EVs were detected with negative-stain TEM in both the EV pool and the concentrated EV pool enriched from the ME/CFS plasma pool (n= 5) and the HC plasma pool (n=5) (Figure 9). In micrograph A, B and C, EVs with the characteristic “cup shaped” TEM artifact morphology was observed. The largest observed EV was ~ 330 nm, while the smallest was ~ 22 nm. In the micrographs there is an overall higher abundance of EVs with diameter below 100 nm. From these micrographs, differences in EVs could not be observed between the cohorts.

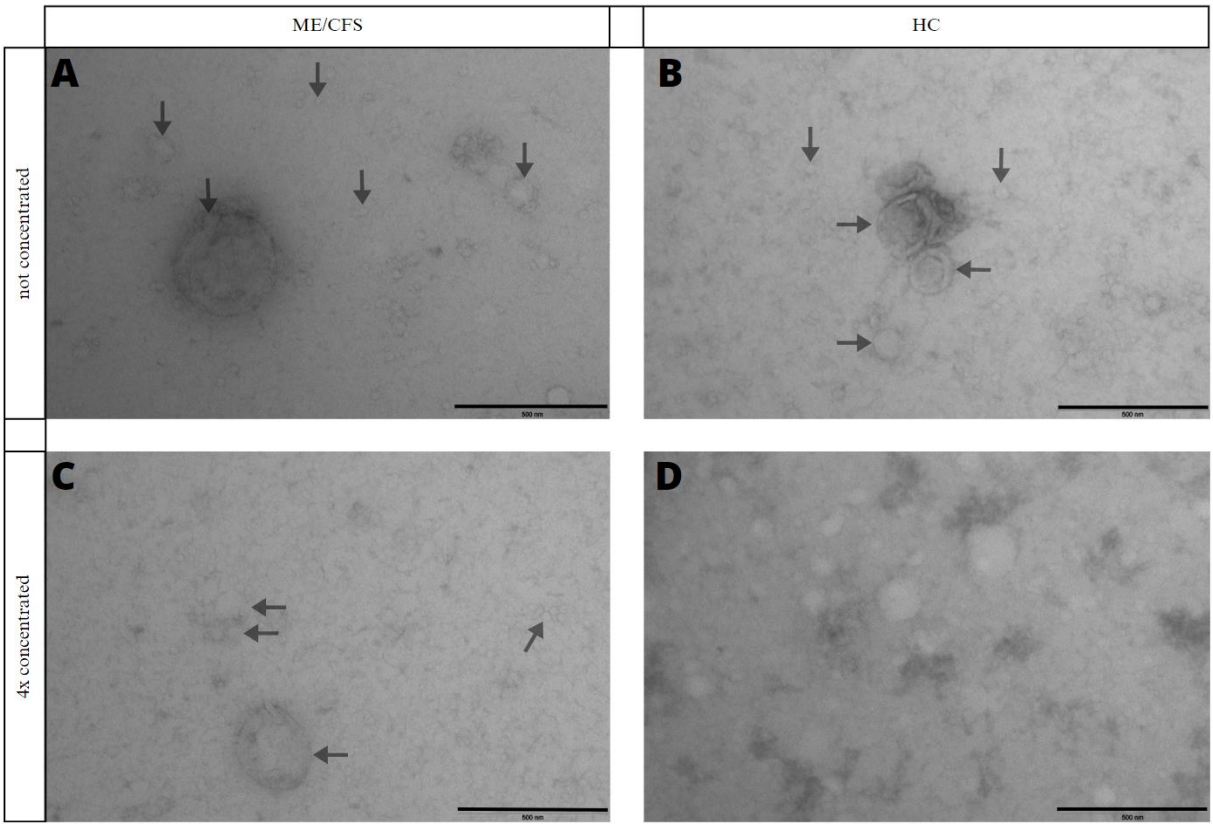

Figure 9: Negative stain transmission electron microscopy of EV pools enriched by size exclusion chromatography from plasma pools of ME/CFS patients (n=5) and HCs (n=5). The scale bars are 500 nm. Each arrow points to the delimiting membrane of a discerned EV. **A**) not concentrated ME/CFS EV pool. **B**) not concentrated HC EV pool. **C**) 4x concentrated ME/CFS EV pool. **D**) 4x concentrated HC EV pool.

4.4.2 Immuno-TEM

CD63-positive EVs were detected in both the ME/CFS and HC EV pools (Figure 10). In the immuno-TEM micrographs presented, the horizontal dark arrows point on CD63-positive EVs, where a wide vertical arrow points to the gold particle attached to the antibody indicating the presence of CD63 on said EV. White arrows point at what is most likely CD63-negative EVs. In line with the western blot analyses (Figure 6), the micrograph showed low abundance of CD63. As previously seen in the micrographs of Figure 9, EVs look intact and smaller EVs with diameter below 100 nm were more abundant.

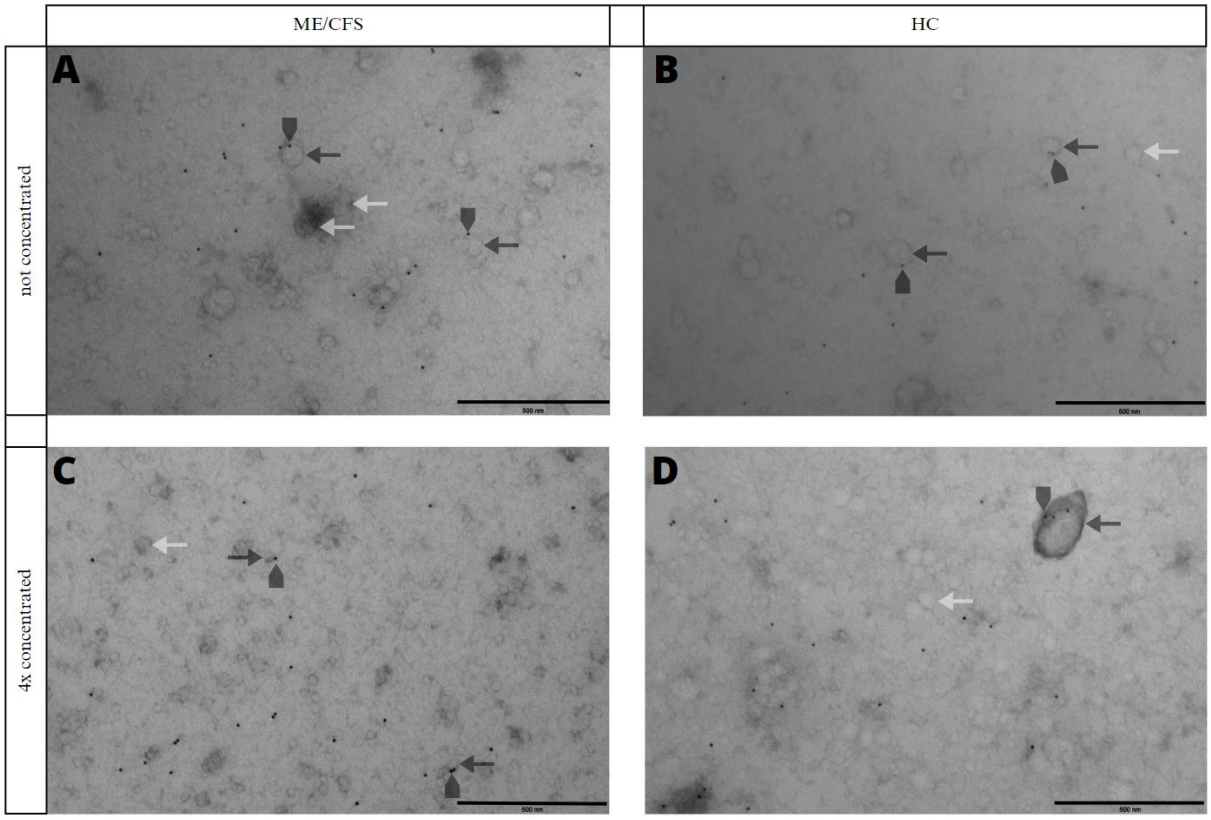

Figure 10: CD63 immuno gold-stained transmission electron micrographs of EV pools of ME/CFS patients (n=5) and HCs (n=5). The scale bars are 500 nm. Dark horizontal arrows indicate CD63-positive EVs, where wide vertical arrows point at gold particle indicating CD63 protein. White arrows point to CD63-negative EVs. **A**) not concentrated ME/CFS EV pool. **B**) not concentrated HC EV pool. **C**) 4x concentrated ME/CFS EV pool. **D**) 4x concentrated HC EV pool.

In the micrographs presented there could not be observed significant differences in the EVs between the ME/CFS- and the HC EV pools (Figure 9 and 10). The presence of clustered EVs were higher in the micrographs of ultrafiltrated EV pools (Figure 9 and 10, C and D).

4.5 EV concentration and -size by nanoparticle tracking analysis

The normality assessment of the NTA data revealed non-normal distribution of mean EV concentration- and mode EV size data with Shapiro-Wilkins normality tests p-values < 0.05 (Table 4). Mean EV size could be considered approximately normally distributed (Table 4), and variances were equal (p = 0.75). Following normality assessment, the EV concentration and -mode size were analyzed with Mann-Whitney U tests, while mean size was analyzed with a two-sample t-test.

Table 4: Test for normal distribution of data from nanoparticle tracking alaysis

	ME/CFS patients (n = 20), p-values*	**HCs (n=20), p-values***
EV concentration	0.0008	0.0000002
Mean EV size	0.8	0.2
Mode EV size	0.003	0.5

* Shapiro-Wilkins normality test

Significant difference in EV concentration was observed between the cohorts (p-value = 0.006) (Figure 11). Concentration of circulatory EVs was higher in the ME/CFS cohort, however, the concentration ranges were large, particularly for the patients, which overlapped with the controls (Table 5 and Figure 11). Hence, the interquartile range of the ME/CFS patients was considerably wider than the HCs, thus the ME/CFS EV concentration data is more dispersed (Figure 11). In both cohorts, EV concentration data was skewed towards higher concentration. There were two ME/CFS outliers, and four HC outliers (Figure 11). Statistical significance remained after removal of outliers (p = 0.002).

Table 5: Summary of EV concetration and -size *of plasma EVs enriched from the ME/CFS cohort (n=20) and HC cohort (n=20).*

	ME/CFS patients (n=20)	**HCs (n=20)**
Mean EV concentration as particles/ml, median (interquartile range)	1.91×10^{10} (3.51×10^{10})	5.47×10^{9} (2.78×10^{9})
Mean EV size in nm, mean ± standard deviation	123.3 ± 11.7	125 ± 12.6
Mode EV size in nm, mean ± standard deviation	97.7 ± 10.7	102.8 ± 15.6

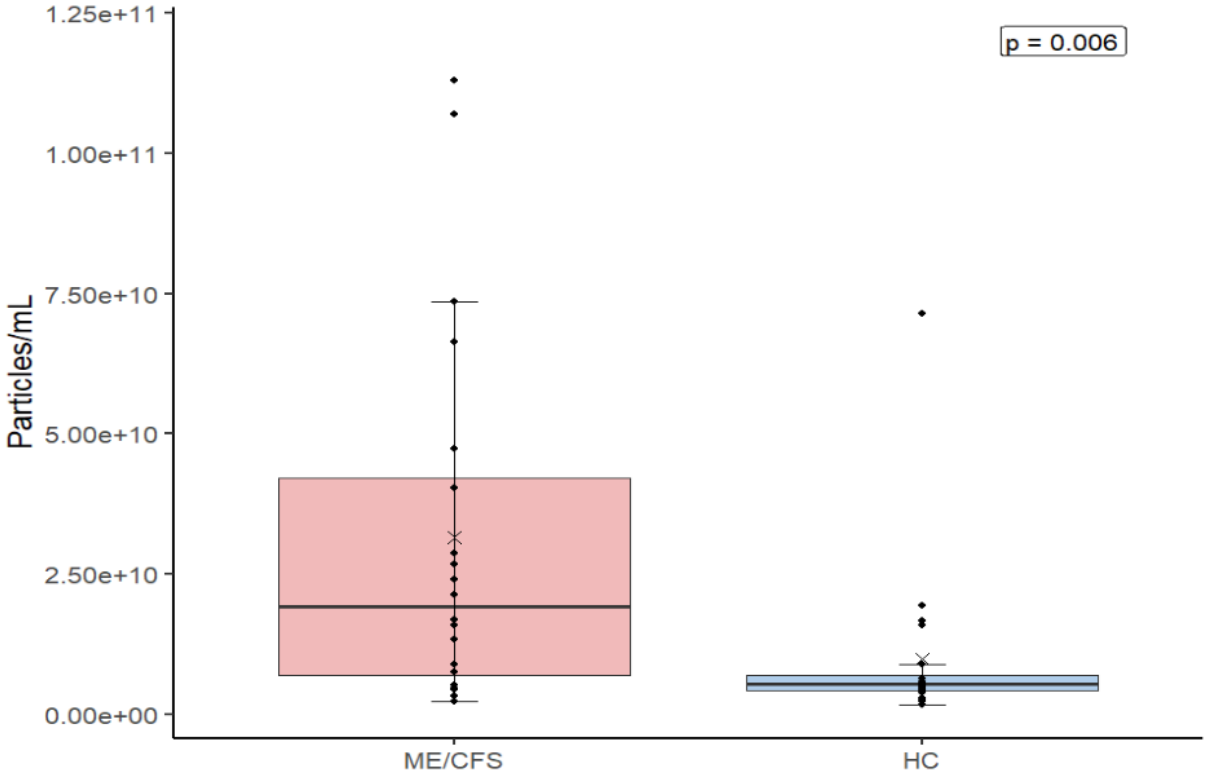

Figure 11: Distribution of mean EV concentration in EV enriched samples *from ME/CFS patients (n=20) and HCs (n=20) quantified by nano particle tracking analysis. The horizontal line within each box indicates median, the box indicates interquartile range, and the cross indicates the mean. Datapoints outside whiskers were considered outliers.*

There could not be observed significant difference in mean- or mode EV size between the two cohorts (p-value > 0.05) (Figure 12). Most detected particles were within 50 – 200 nm in diameter.

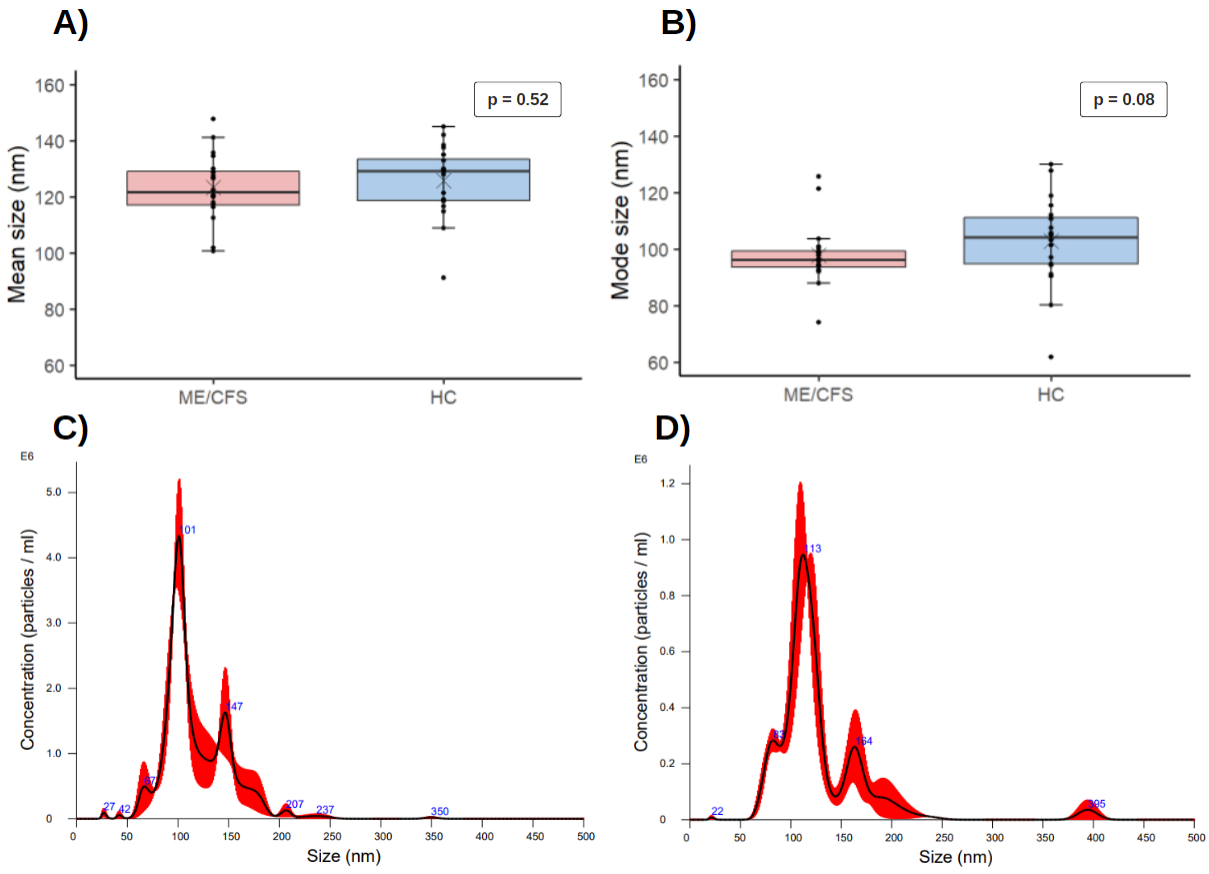

Figure 12: EV size in patients and controls measured by nanoparticle tracking analysis (NTA). *Distribution of **A**) mean EV size and **B**) mode EV size in EV enriched samples from ME/CFS cohort (n=20) and HC cohort (n=20). NTA graph of **C**) one ME/CFS patient **D**) and their matched control.*

4.6 Proteomic profiling of EV enriched samples

Analysis of the mass spectrometry data identified 663 unique proteins in the EV enriched samples over both cohorts. Of the 663 detected proteins, 602 of the proteins had attached gene names. When compared with human protein entries in Vesiclepedia, 535/602 overlapped (Figure 13). The majority of the 67 non-overlapping proteins were immunoglobulins.

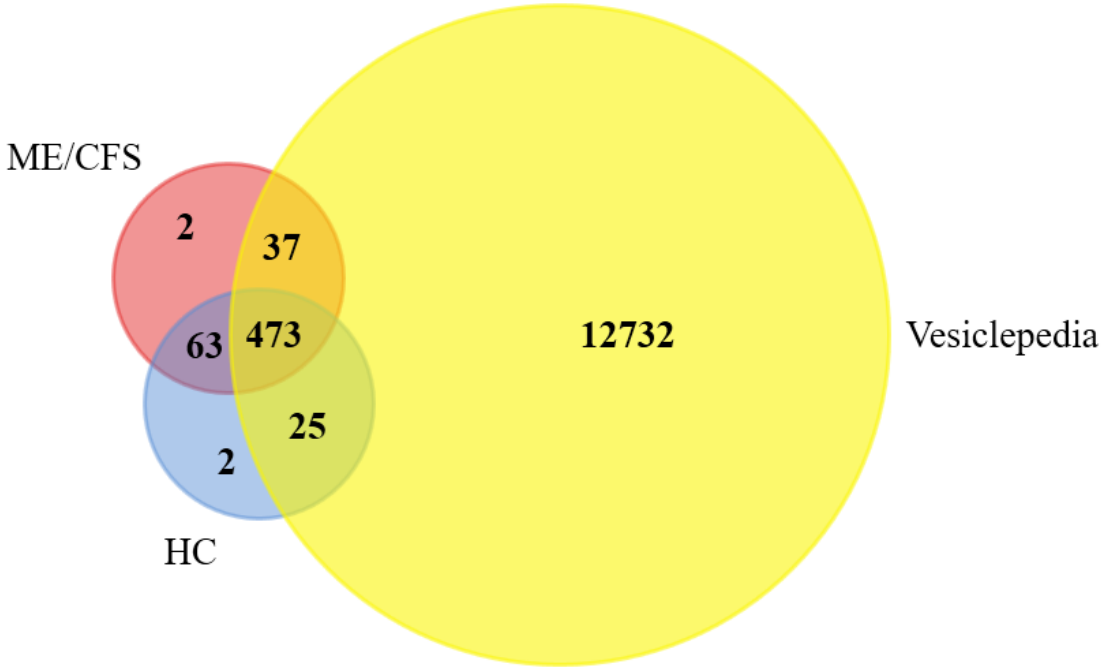

Figure 13: Venn diagram of human protein entries to Vesiclepedia and gene names of detected proteins in EV enriched samples from the ME/CFS cohort (n=20) and 20 HCs (n=20).

Of the 663 detected proteins, 41 were exclusively detected in the ME/CFS patients and 29 were exclusively detected in the HCs (Figure 14).

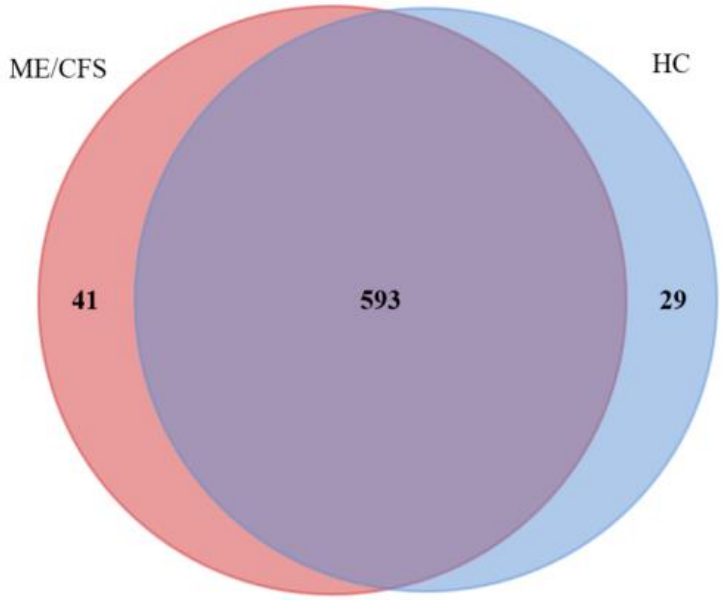

Figure 14: Venn diagram of proteins detected in EV enriched samples from the ME/CFS cohort (n=20) and HCs (n=20).

Notably, 278/634 and 267/622 proteins were detected in all subjects of the ME/CFS and HC cohort respectively (Figure 15, A and B). Of the exclusively detected proteins in each cohort most were detected in few individuals (Figure 15, E and F). If proteins had to be to be detected in minimum 50% of the subjects to be considered detected in the cohort, all exclusively detected protein would have been discarded. Studying which subjects the cohort exclusive protein were detected in revealed an even distribution (Figure 15, C and D), except one subject in the ME/CFS cohort in which 15 were detected. This subject accounted for detection of 11/41 ME/CFs cohort exclusive proteins.

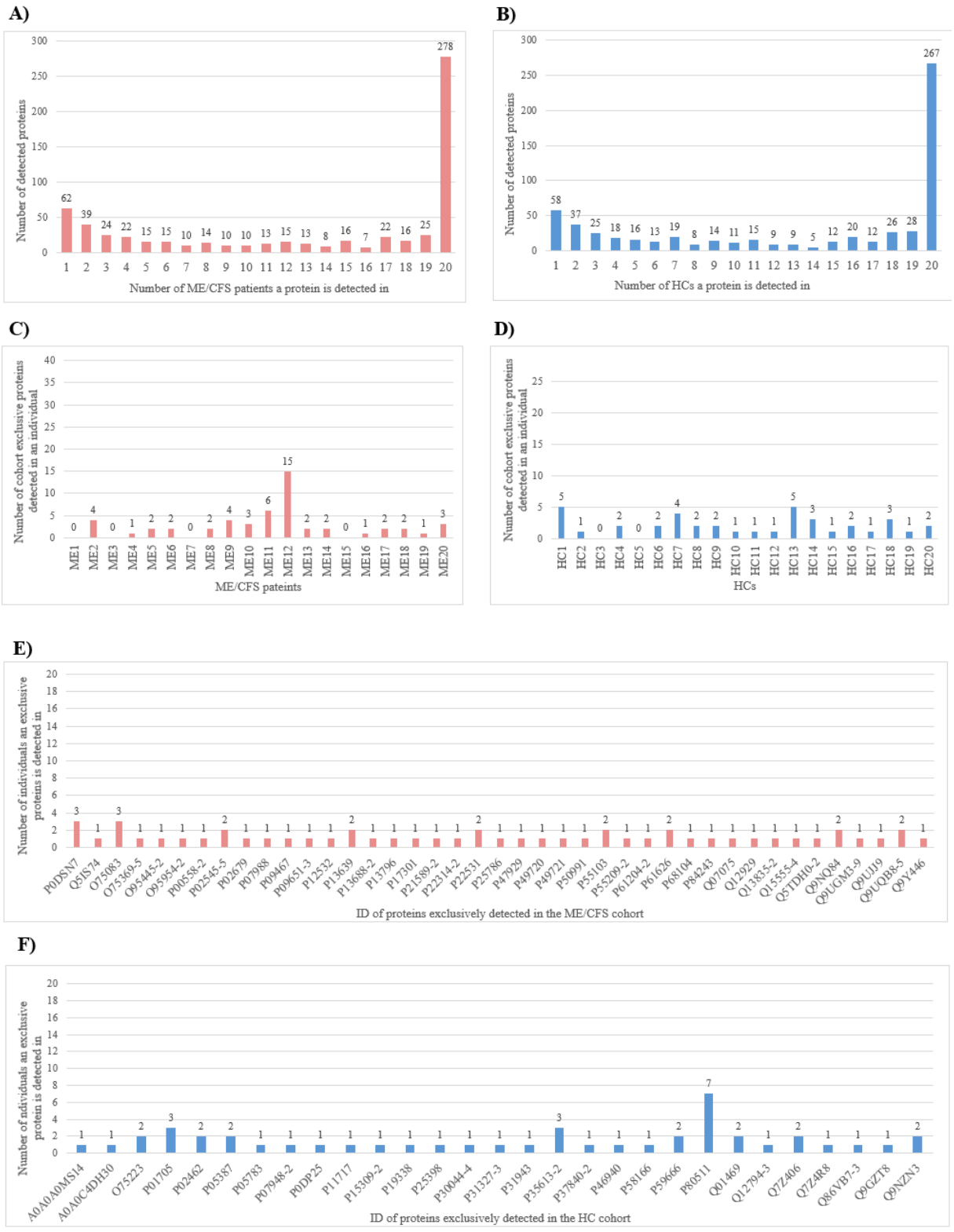

Figure 15: Number of subjects each protein was detected in with label free mass spectrometry, *in the* ***A****) ME/CFS cohort (n=20) and* ***B****) HC cohort (n=20).* ***C****) and* ***D****) distribution of cohort exclusive protein detected in each subject of each cohort.* ***E****) and* ***F****) Number of subjects within each cohort each cohort exclusive protein was detected in.*

5. Discussion

The primary aim of this project was to study EVs in ME/CFS and assess their potential as biomarkers for the disease. Through using EV relevant methods including SEC, western blotting, NTA, TEM and mass spectrometry, our study investigated EV concentration, -size, -morphology and protein cargo in patient- and HC derived samples.

5.1 Is SEC an appropriate EV isolation method?

No gold-standard technique for EV isolation is established, and the different methods in use enrich for different EV populations from the same material (112). Currently, the choice of a method is a compromise between EV recovery and purity and should therefore involve considerations of source material and downstream applications (46). Furthermore, costs and availability of equipment might be relevant. Differential ultracentrifugation was the first method for EV isolation and is still the most widely used (113). Therefore, the method is well-established, however it has limitations regarding reproducibility, purity, and may cause aggregation of EVs (142). Over time, ultracentrifugation has been replaced by less laborious and more gentle isolation techniques, including SEC which has become the second most common method (113). One limitation with using SEC or ultracentrifugation that separates based on density and/or size over a more size inclusive technique, such as filtration or precipitation, is that potential biologically significant EVs of different size would be excluded. Thus, the findings in each study should be applied to the population of EVs the protocol in use yielded. Considering the size ranges commonly assigned to each EV subgroup in the literature our SEC isolated population of small EVs (sEVs), with diameter of 50-200 nm, is assumed to primarily consist of exosomes (30-150 nm) and small microvesicles (100-1000 nm) (48). However, size is not an accurate estimate of subgroups, and as subgroups-specific markers are not established this assumption is only speculative. In the context of our aim of biomarker discovery, an EV population primarily consisting of exosomes was compatible since the sorting of protein cargo to exosomes during biogenesis is thought to be non-random, thus exosome cargo is often of focus in EV related biomarker research (63). However, a less specific isolation method may be a better choice for studies wanting to analyze a more accurate representation of the whole range of EVs in blood, though this would yield less pure samples.

A gentle and more specific variation of ultracentrifugation, density gradient centrifugation, could be coupled to SEC or ultracentrifugation to increase sample purity, but at the cost of EV recovery (46, 115). Regarding the aim of biomarker discovery, further purification may exclude significant EV-populations. However, it might also reveal signals that would otherwise be overshadowed in the less specific EV enrichments, such as disease specific proteins from small exosomes being diluted by protein cargo of larger microvesicles in label-free proteomic analyses. Thus, the use and pairing of several isolation methods, or separation of EV populations before analysis, might be beneficial to biomarker discovery.

Notably, the various EV isolation methods will affect the population of EVs and non-EV components of the final isolate. Thus, in choosing a method researchers should consider their aims, the source material, in which downstream analyses the EV samples will be used, availability of equipment, efficiency, and costs. Although SEC fails to completely isolate plasma EVs from other plasma components with overlapping size, such as lipoproteins, it has many desirable traits for EV isolation and biomarker discovery that is complementary to our aims, material, equipment, and budget (143). Namely, it recovers a sufficient amount of EVs from a small volume of material while yielding a relatively clean sample, allows for consistent isolation, is gentle, and shows great potential for clinical implementation (117, 144).

5.2 Can source material and processing influence results?

Processing, handling, and choice of the EV source material will influence the recovery of EVs (46). Thus, pre-analytic processing is described thoroughly in the methods section of this thesis. Allowing clotting of blood samples after collection, in processing of serum, will cause secretion of platelet derived EVs (111, 145). Hence, an anticoagulant was added to the ex vivo sample, yielding plasma, to minimize the introduction of artifact EVs that would alter the in vivo EV composition and potentially dilute the signal of EVs from pathological cells. Previous studies have shown EDTA to be sufficient at inhibiting platelets (111). Furthermore, storage of both plasma and isolated EV samples can influence the EVs. Thus, blood was processed shortly after collection, and plasma was stored at -80°C, which is in line with recommendations (142). Still, it cannot be excluded that some sample processing variation may have occurred, potentially affecting our results.

A study reported aggregation and a 25% increase in diameter of isolated airway EVs stored for four days at -80℃ compared to freshly isolated sample (146). Thus, EV samples were delivered fresh to NTA, as freezing may affect NTA results both due to increased diameter and since the aggregates will be counted as one large particle (147).

Another issue to consider is what tissue is a relevant EV source for the disease being studied. With evidence of inflammation in the central nervous system of ME/CFS patients (148), it could be argued that cerebrospinal fluid may be a more biologically relevant biofluid to study over blood. Yet, in the light of biomarker discovery, the minimally invasive nature of blood collection is central.

In conclusion there are many variables in the processing, handling and storage of both source material and isolated EV samples that may affect the outcome. Hence, the current lack of standardization makes it difficult to compare findings. Notably, our plasma- and EV samples were frozen in small aliquots to avoid re-freezing, and samples from NTA and TEM were delivered freshly isolated to avoid manipulation of EV size due to freezing.

5.3 Did we enrich for EVs?

The presence of EVs and co-isolates must be assessed through characterization of the pooled SEC fractions (46). Optimized western blot experiments validated enrichment of EVs through detection of EV markers CD9, CD63 and TSG101. Surprisingly, the bands representing CD9 detection appeared weaker on the blot with the concentrated EV pools than the non-concentrated pools. This was not caused by the difference in exposure time, as the observed difference remained when comparing images with the same exposure time. The weaker bands could have been caused by inaccurate loading of the wells, but after further inspection of the blot, the ladder also appeared weaker. Thus, it is likely that the appearance of a weaker CD9 band on the blot with concentrated samples was caused by overshadowing from the unexpected band at approximately 200 kDa. The origin of the band is unknown, however it could be caused by insufficient denaturation or reducing of the sample, or possibly overloading of the wells as 40 µl was applied and the sample is concentrated. Nevertheless, the presence of CD9 is clearly detected in EV pools from both cohorts.

Since CD63 is a glycoprotein, it was not unexpected that the band detecting CD63 appeared as a smear, as reported by other studies of plasma derived EVs (119, 149). Surprisingly,

CD63 was only faintly detected in the non-concentrated EV pool despite using the same antibody concentrations as in the CD9 detection experiment. Further optimization might have improved the detection of CD63, such as increasing the primary antibody concentration. The stronger bands on the blot with protein from concentrated EV pools support the success of increasing EV concentration by ultrafiltration. The faint detection of CD63 is in line with our immuno-TEM micrographs where surprisingly few gold particles indicating CD63 proteins were observed. Together, these findings indicate presence of few CD63-positive EVs in our EV enriched samples. Supporting this, a recent single-EV study from our research group detected tetraspanin expression on sEVs isolated with SEC from plasma of rheumatoid arthritis patients and controls and found that few sEVs appeared to carry CD63 in both cohorts (150).

Unexpectedly, bands detecting TSG101 appeared above the molecular weight of 50 kDa. The polyacrylamide gel percentage is known to influence the size separation of proteins (151). Notably, the 4-20% gradient gel we used does not separate proteins of TSG101's molecular weight well, which might have caused the bands to appear higher than expected. Ideally a 10% gel would have been used, however this was not available at the time of conducting the western blot experiments. If given time for additional optimization primary and secondary antibodies would have been further diluted as protein detection was strong at short exposure time. The insufficient dilution of the secondary antibody could have contributed to the high background and spots on the blot.

The detection of albumin confirms presence of non-EV co-eluates in the EV enriched samples. After a study observing EV loss following lipoprotein depletion in plasma prior to NTA, it is currently unknown whether the co-eluates are as previously labelled, "contaminants", or in fact a part of the functional EV corona (73, 75, 152). If the latter is the case, the co-eluates could in line with the canonical EV cargo be significant in biomarker discovery. Moreover, if albumin is associated with the EVs, this could explain why the band detecting albumin in the ME/CFS pool appeared stronger than in the HC pool, since the EV concentration was higher in the ME/CFS EV samples.

If provided more time, optimization of western blots would have been continued further. The consistent problem of dark spotting on the membranes was not resolved but believed to be caused by incomplete dissolving of the blocking reagents, inadequate dilution of the secondary antibody, or contaminants. Ideally, antibody concentrations would have been

further adjusted. However, further optimization was not necessary as the western blots were not intended to be used for quantitative analysis, but rather to validate the presence of EV- and non-EV markers in our EV enriched samples.

Characterization of EVs with TEM did not reveal any morphological differences in EVs between the two cohorts. Notably, this does not confirm that there is no difference, but it could not be observed in these specific sections. In general, achieving clear micrographs of plasma derived EVs proved difficult, and the final micrographs had dark backgrounds due to several layers of EVs. Whether the EV pools or the concentrated EV pools would yield the best micrographs was of interest during the TEM optimization. From the final micrographs the pools appear similar except for a higher presence of EV aggregation in the concentrated pools. The presence of EVs was confirmed by immunogold labeling of CD63. Detection of CD63 was unexpectedly low which complicated distinguishing of EV from non-EV components in the micrographs. This correlates with the faint CD63 bands on the western blots. Low labeling of CD63 could have occurred due to low presence of EVs in our samples, however this is not likely as the great majority of LC-MS/MS-identified proteins overlapped with Vesiclepeida, thus these have previously been detected as EV associated proteins. Considering our western blot analysis and the single-sEV study which captured fewer sEV expressing CD63 than CD9 (150), immunogold labeling of CD9 or other EV markers, rather than CD63, might have been more efficient in assessing sample purity.

Due to SEC being performed equally to enrich for EVs from all plasma samples, we assume the validation of EVs with western blotting and TEM in the representative EV pools to be transferable to validation of EVs in the EV enriched samples from all ME/CFS subjects (n=20) and HCs (n=20). This assumption is further supported by the analysis of LC-MS/MS- and NTA data from all participants, since the majority of identified proteins overlapped with registered EV proteins in Vesiclepedia and the presence of EV-sized particles was confirmed.

In conclusion, the successful detection of three established EV markers by western blot (46), observation of EVs with TEM, identification of registered EV proteins with LC-MS/MS and quantification of EV-sized particles with NTA confirms successful enrichment of EVs in our EV enriched samples isolated with SEC. Equally, the detection of albumin confirms presence of co-eluates, and possibly contaminants, in our EV enriched samples which should be considered in the interpretations of our results.

5.4 Characterization of sEVs in ME/CFS patients revealed difference in EV concentration but not EV size

Supporting the findings of previous ME/CFS EV studies (119-122), our results indicate a significantly increased number of circulatory EVs in ME/CFS patients compared to healthy subjects. The previous studies used precipitation-based isolation for enrichment of EVs from serum (119) or plasma (120-122) and quantified EV enriched samples using NTA (119, 120, 122), or flow cytometry (121). Taken together, the observation of increased circulatory EV concentration in patients has been replicated in several cohorts using different methods for sample processing, isolation, and quantitation. However, one study did not corroborate these findings (123). Due to overlap in sEV concentration between patients and HCs, and observations of increased EV concentration in other patient groups (126, 127), increased circulatory sEV concentration does not qualify as an ME/CFS specific diagnostic biomarker. Nevertheless, it does suggest an abnormality in EV secretion. The observation further supports established hypotheses on the pathogenesis of ME/CFS, as increased EV secretion has previously been observed in response to both inflammation (153) and tissue hypoxia (154).

Contrary to the findings of two previous studies (119, 120), our results did not reflect a significant difference in EV size between cohorts. Eminently, our findings are reserved for the population of sEVs our plasma processing and isolation method yielded, not all circulatory EVs. The two previous studies enriched for EVs with precipitation-based isolation from serum (119) or plasma (120). Difference in isolation technique might contribute to our differing findings. Additionally, these studies had small sample sizes of ten patients and five controls, and fifteen patients and fifteen controls, respectively. Non-significant difference in circulatory sEV size in ME/CFS patients has previously been observed in a study with participant number equal to ours (122).

The NTA measurement might not have captured all particle as it is less sensitive at detecting particles below 70 nm (155). This could explain why a larger proportion of EVs and non-EV particles with diameter below 70 nm was observed with TEM, relative to what was expected from the NTA graphs. This is supported by the single-EV study, where the estimated mean diameter of EVs expressing CD9, CD63, and/or CD81 was 62 nm (±17 nm) in samples enriched from control plasma through the same SEC protocol as described in this thesis (150).

Thus, the NTA data may not report the true EV concentration and -mean diameter in the EV enriched samples, however the technique is still suitable for use in relative comparisons (156). Furthermore, the NTA results did confirm presence of EV sized particles which further validates presence of EVs in the EV enriched samples.

The dynamic nature of the secretome could further limit our analyses as EV secretion and -cargo may be affected by demographics (157), exercise (158), fasting state (159) and potentially time of day the blood sample was collected. Furthermore, potential confounding effects in biomedical studies on ME/CFS naturally include the lifestyle of patients. As a consequence of debilitating symptoms including post exertional malaise and pain, patients are more likely to be sedentary. Thus, potential differences in lifestyle of patients and controls, regardless of disease state, may have influenced our findings. Due to the dynamic secretome, some variance in EV concentration was expected within both cohorts. However, the spread was considerably wider in the ME/CFS cohort. The difference in spread between the cohorts may have influenced the results of the statistical tests (160). In addition, the wide spread of EV concentration suggests heterogeneity within the ME/CFS cohort. This could be caused by the difference in symptoms and disease severity among patients (1), as some of the ME/CFS subjects included in our study were reported as bedridden at time of blood collection. Time elapsed since disease onset was not provided but could contribute to the spread and overlap with HCs, as the uniqueness of plasma immune signatures in ME/CFS patients previously have been shown to inversely correlate with disease duration (161). The observed variance in EV concentration in the cohort could also have been caused if ME/CFS, as has been suggested, consist of several subgroups with different pathogenic mechanisms that affect EV secretion to a varying extent. However, the large variance could be a result of inclusion of misdiagnosed patients, or comorbidities.

Notably, all EV concentration outliers had BMI ≥ 24. The outlier with the highest EV concentration in the HC cohort is the HC with the highest BMI of 36, which is within the obesity range. However, a patient with similar BMI had concentration below the median of the ME/CFS group. Overall BMI was higher in the HCs than the ME/CFS patients and still EV concentration was significantly increased in the ME/CFS cohort. Thus, EV concentration seems to rely more on disease state than BMI. If more time was available, a correlation analysis between EV concentration and demographics including BMI could have been performed.

5.5 An ME/CFS specific sEV protein profile was not identified

To our knowledge, this is the largest ME/CFS EV proteomics study to date, still the results are limited by the small sample sizes. Proteins exclusively identified in each cohort were detected in few subjects and did not contribute to differences between cohorts as much as interindividual variability. Notably, the "cohort exclusiveness" of the proteins can not be established by our analysis as the LC-MS/MS was label-free and intensities were normalized. Thus, this method limits our analysis since it can not confirm the absence of a protein in a sample. Hence, any speculations on cohort exclusive protein must be replicated using targeted methods, e.g. mass spectrometry-based targeted proteomics or enzyme-linked immunosorbent assay.

In terms of future studies, comparison of EV associated proteins should be extended to include differential expression analysis. Ideally this would have been performed in the current study but was halted due to time limitations. Comparing the EV proteome from three patients and three controls Eguchi et al. discovered 134 differentially expressed proteins, of which actin network proteins were prominent (121). The increased expression of actin network proteins remained when comparing the EV sample proteome from cohorts of four ME/CFS-, depression-, and idiopathic chronic fatigue patients (121). Despite few subjects, differential expression analysis of EV proteome from ME/CFS shows potential in biomarker discovery and will be performed following this project. However, the current stage of our proteomic analysis could not reveal any significant difference in EV associated proteins between samples from patients and HCs.

5.6 Assessment of circulatory EVs as a source of potential ME/CFS biomarkers

In this study we have shown that EVs can easily be enriched from non-invasive samples like blood plasma and can be used methods for characterization, and proteomic analyses. However, the full analysis of circulatory EVs as potential source of biomarkers for ME/CFS was not completed during this project, as differential expression analysis of proteomic data was not performed. EVs had similar size and morphology between cohorts, but the concentration of EVs was significantly elevated in patients. Increased EV concentration

indicates altered EV secretion in ME/CFS patients. Thus, EVs pose as a potential source of ME/CFS biomarkers. This should be further investigated in larger cohorts and include more extensive analysis of cargo, firstly analyzing protein- and RNA cargo.

5.7 Considerations for future studies

Adjustments and additional analyses could have been performed to improve the study of EVs in ME/CFS and their potential as biomarkers. Assessment of sample purity could have been extended to include detection of lipoprotein markers, in addition to albumin. Additionally, a more abundant surface EV marker could have been labeled during immuno-TEM to improve distinguishing of EVs from non-EV structures. From our western blot experiments, it is likely immunogold labelling of CD9 would have been preferable, alternatively labeling of several surface EV markers.

In addition to general EV markers, cell specific markers could have been investigated. The plea for increased standardization within the EV research field is hoped to allow establishment of EV subtype-, donor cell-, and target cell type markers. Some origin markers are currently in use and could have been investigated to determine and compare from which cells EVs were secreted. Future determination of both origin and target could increase the insight into EVs potential role in ME/CFS and should be conducted following the establishment of these markers.

Based on our findings of increased EV concentration in addition to increased albumin in the ME/CFS EV pool, future EV studies may benefit from avoiding treatment with proteinases, e.g., proteinase K, as the EV surface associated proteins and -corona may be of relevance.

The analysis of EV associated proteins revealed a high number of proteins. Differential expression analysis should be completed to further determine the potential of EV associated proteins as ME/CFS biomarkers. Furthermore, “cohort exclusive” proteins should be replicated with targeted methods for more accurate quantitation. Future studies on biomarker discovery may benefit from analyzing additional cargo including EV associated RNAs.

Present ME/CFS biomedical studies naturally include the lifestyle of patients as a potential confounder. Hence, future studies with the aim to study pathogenic mechanisms in ME/CFS should consider the inclusion of sedentary controls, to limit the effect of low physical activity in patients. Following the identification of a potential EV biomarker for ME/CFS, replication

should include disease cohorts, in particular of diseases with symptom overlap to ME/CFS. Furthermore, future studies may benefit from separating ME/CFS cohorts by disease severity and/or duration both to investigate their respective effects on EV secretion, and potentially limit the great variance observed in this thesis which may disturb statistical tests.

Finally, the findings presented in this study should be replicated in larger datasets. Additionally, all samples analyzed were from females collected in Norway. Future studies should be expanded to include male participants and findings should be replicated in subjects from several populations. Investigation of larger cohorts with samples from several populations will be made easier through further development of efficient EV methods, and standardization between biobanks regarding processing and handling of samples for EV research.

6. Conclusion

We characterized circulatory EVs from ME/CFS patients with the aim to assess their potential as minimally invasive biomarkers for ME/CFS. Full assessment was beyond the scope of this thesis, as complete analysis of EV associated proteins was not performed within the time frame of this thesis. EVs were successfully enriched from plasma of patients and HCs with size exclusion chromatography, as confirmed by detection of EV markers with western blotting and observation of EVs with TEM. Through analysis of NTA data, we confirmed previous findings of elevated EV levels in samples from ME/CFS patients compared to HCs. This observation indicates that EVs may play a role in ME/CFS and is further a testimony to the physical nature of the illness. However, the lifestyle and/or heterogeneity of the patient group poses as potential confounders. Great variation in EV concentration was observed between patients, and significant differences in EV size and -morphology between patients and HCs could not be observed. LS-MS/MS revealed few “cohort exclusive” proteins, that might reflect interindividual variability. However, proteomic analysis was not completed since differential expression of EV associated proteins was not investigated.

In conclusion, EV enrichment and characterization were successfully validated and optimized, respectively, thus providing a good basis for future EV studies. Even though a potential biomarker could not be suggested at this stage, the current findings hint at an altered EV secretion in ME/CFS patients, which strengthens their potential as a source of biomarkers for the disease. Our finding should motivate further EV studies in ME/CFS, as the discovery of biomarkers for ME/CFS is urgently needed.

References

1. Deumer US, Varesi A, Floris V, Savioli G, Mantovani E, Lopez-Carrasco P, et al. Myalgic Encephalomyelitis/Chronic Fatigue Syndrome (ME/CFS): An Overview. J Clin Med. 2021;10(20).
2. Cortes Rivera M, Mastronardi C, Silva-Aldana CT, Arcos-Burgos M, Lidbury BA. Myalgic Encephalomyelitis/Chronic Fatigue Syndrome: A Comprehensive Review. Diagnostics (Basel). 2019;9(3).
3. Fluge Ø, Tronstad KJ, Mella O. Pathomechanisms and possible interventions in myalgic encephalomyelitis/chronic fatigue syndrome (ME/CFS). The Journal of Clinical Investigation. 2021;131(14).
4. Pheby DFH, Friedman KJ, Murovska M, Zalewski P. Turning a Corner in ME/CFS Research. Medicina (Kaunas). 2021;57(10).
5. Bested AC, Marshall LM. Review of Myalgic Encephalomyelitis/Chronic Fatigue Syndrome: an evidence-based approach to diagnosis and management by clinicians. Rev Environ Health. 2015;30(4):223-49.
6. Falk Hvidberg M, Brinth LS, Olesen AV, Petersen KD, Ehlers L. The Health-Related Quality of Life for Patients with Myalgic Encephalomyelitis / Chronic Fatigue Syndrome (ME/CFS). PLoS One. 2015;10(7):e0132421.
7. Committee on the Diagnostic Criteria for Myalgic Encephalomyelitis/Chronic Fatigue S, Board on the Health of Select P, Institute of M. The National Academies Collection: Reports funded by National Institutes of Health. Beyond Myalgic Encephalomyelitis/Chronic Fatigue Syndrome: Redefining an Illness. Washington (DC): National Academies Press (US)

8. Brurberg KG, Fønhus MS, Larun L, Flottorp S, Malterud K. Case definitions for chronic fatigue syndrome/myalgic encephalomyelitis (CFS/ME): a systematic review. BMJ Open. 2014;4(2):e003973.
9. Fukuda K, Straus SE, Hickie I, Sharpe MC, Dobbins JG, Komaroff A. The chronic fatigue syndrome: a comprehensive approach to its definition and study. International Chronic Fatigue Syndrome Study Group. Ann Intern Med. 1994;121(12):953-9.
10. Carruthers BM, Jain AK, De Meirleir KL, Peterson DL, Klimas NG, Lerner AM, et al. Myalgic Encephalomyelitis/Chronic Fatigue Syndrome. Journal of Chronic Fatigue Syndrome. 2003;11(1):7-115.
11. Carruthers BM, van de Sande MI, De Meirleir KL, Klimas NG, Broderick G, Mitchell T, et al. Myalgic encephalomyelitis: International Consensus Criteria. J Intern Med. 2011;270(4):327-38.
12. Lim E-J, Ahn Y-C, Jang E-S, Lee S-W, Lee S-H, Son C-G. Systematic review and meta-analysis of the prevalence of chronic fatigue syndrome/myalgic encephalomyelitis (CFS/ME). Journal of Translational Medicine. 2020;18(1):100.
13. Bakken IJ, Tveito K, Gunnes N, Ghaderi S, Stoltenberg C, Trogstad L, et al. Two age peaks in the incidence of chronic fatigue syndrome/myalgic encephalomyelitis: a population-based registry study from Norway 2008-2012. BMC Med. 2014;12:167.
14. Chu L, Valencia IJ, Garvert DW, Montoya JG. Onset Patterns and Course of Myalgic Encephalomyelitis/Chronic Fatigue Syndrome. Front Pediatr. 2019;7:12.
15. Prins JB, van der Meer JW, Bleijenberg G. Chronic fatigue syndrome. Lancet. 2006;367(9507):346-55.
16. Albright F, Light K, Light A, Bateman L, Cannon-Albright LA. Evidence for a heritable predisposition to Chronic Fatigue Syndrome. BMC Neurol. 2011;11:62.
17. Buchwald D, Herrell R, Ashton S, Belcourt M, Schmaling K, Sullivan P, et al. A twin study of chronic fatigue. Psychosom Med. 2001;63(6):936-43.
18. Hickie IB, Bansal AS, Kirk KM, Lloyd AR, Martin NG. A twin study of the etiology of prolonged fatigue and immune activation. Twin Res. 2001;4(2):94-102.

19. Hajdarevic R, Lande A, Rekeland I, Rydland A, Strand EB, Sosa DD, et al. Fine mapping of the major histocompatibility complex (MHC) in myalgic encephalomyelitis/chronic fatigue syndrome (ME/CFS) suggests involvement of both HLA class I and class II loci. Brain, Behavior, and Immunity. 2021;98:101-9.
20. Lande A, Fluge Ø, Strand EB, Flåm ST, Sosa DD, Mella O, et al. Human Leukocyte Antigen alleles associated with Myalgic Encephalomyelitis/Chronic Fatigue Syndrome (ME/CFS). Sci Rep. 2020;10(1):5267.
21. Loebel M, Strohschein K, Giannini C, Koelsch U, Bauer S, Doebis C, et al. Deficient EBV-specific B- and T-cell response in patients with chronic fatigue syndrome. PLoS One. 2014;9(1):e85387.
22. Rasa S, Nora-Krukle Z, Henning N, Eliassen E, Shikova E, Harrer T, et al. Chronic viral infections in myalgic encephalomyelitis/chronic fatigue syndrome (ME/CFS). J Transl Med. 2018;16(1):268.
23. Cameron B, Flamand L, Juwana H, Middeldorp J, Naing Z, Rawlinson W, et al. Serological and virological investigation of the role of the herpesviruses EBV, CMV and HHV-6 in post-infective fatigue syndrome. J Med Virol. 2010;82(10):1684-8.
24. Loebel M, Eckey M, Sotzny F, Hahn E, Bauer S, Grabowski P, et al. Serological profiling of the EBV immune response in Chronic Fatigue Syndrome using a peptide microarray. PLoS One. 2017;12(6):e0179124.
25. Rasa-Dzelzkaleja S, Krumina A, Capenko S, Nora-Krukle Z, Gravelsina S, Vilmane A, et al. The persistent viral infections in the development and severity of myalgic encephalomyelitis/chronic fatigue syndrome. J Transl Med. 2023;21(1):33.
26. Hickie I, Davenport T, Wakefield D, Vollmer-Conna U, Cameron B, Vernon SD, et al. Post-infective and chronic fatigue syndromes precipitated by viral and non-viral pathogens: prospective cohort study. BMJ. 2006;333(7568):575.
27. Rivas JL, Palencia T, Fernández G, García M. Association of T and NK Cell Phenotype With the Diagnosis of Myalgic Encephalomyelitis/Chronic Fatigue Syndrome (ME/CFS). Front Immunol. 2018;9:1028.
28. Bradley AS, Ford B, Bansal AS. Altered functional B cell subset populations in patients with chronic fatigue syndrome compared to healthy controls. Clin Exp Immunol. 2013;172(1):73-80.
29. Chang CM, Warren JL, Engels EA. Chronic fatigue syndrome and subsequent risk of cancer among elderly US adults. Cancer. 2012;118(23):5929-36.
30. Marshall-Gradisnik S, Huth T, Chacko A, Johnston S, Smith P, Staines D. Natural killer cells and single nucleotide polymorphisms of specific ion channels and receptor genes in myalgic encephalomyelitis/chronic fatigue syndrome. Appl Clin Genet. 2016;9:39-47.
31. Brenu EW, van Driel ML, Staines DR, Ashton KJ, Hardcastle SL, Keane J, et al. Longitudinal investigation of natural killer cells and cytokines in chronic fatigue syndrome/myalgic encephalomyelitis. J Transl Med. 2012;10:88.
32. Theorell J, Bileviciute-Ljungar I, Tesi B, Schlums H, Johnsgaard MS, Asadi-Azarbaijani B, et al. Unperturbed Cytotoxic Lymphocyte Phenotype and Function in Myalgic Encephalomyelitis/Chronic Fatigue Syndrome Patients. Front Immunol. 2017;8:723.
33. Fluge Ø, Bruland O, Risa K, Storstein A, Kristoffersen EK, Sapkota D, et al. Benefit from B-lymphocyte depletion using the anti-CD20 antibody rituximab in chronic fatigue syndrome. A double-blind and placebo-controlled study. PLoS One. 2011;6(10):e26358.
34. Fluge Ø, Risa K, Lunde S, Alme K, Rekeland IG, Sapkota D, et al. B-Lymphocyte Depletion in Myalgic Encephalopathy/ Chronic Fatigue Syndrome. An Open-Label Phase II Study with Rituximab Maintenance Treatment. PLoS One. 2015;10(7):e0129898.
35. Fluge Ø, Rekeland IG, Lien K, Thürmer H, Borchgrevink PC, Schäfer C, et al. B-Lymphocyte Depletion in Patients With Myalgic Encephalomyelitis/Chronic Fatigue Syndrome: A Randomized, Double-Blind, Placebo-Controlled Trial. Ann Intern Med. 2019;170(9):585-93.
36. Tanaka S, Kuratsune H, Hidaka Y, Hakariya Y, Tatsumi KI, Takano T, et al. Autoantibodies against muscarinic cholinergic receptor in chronic fatigue syndrome. Int J Mol Med. 2003;12(2):225-30.

37. Loebel M, Grabowski P, Heidecke H, Bauer S, Hanitsch LG, Wittke K, et al. Antibodies to β adrenergic and muscarinic cholinergic receptors in patients with Chronic Fatigue Syndrome. Brain Behav Immun. 2016;52:32-9.
38. Scheibenbogen C, Loebel M, Freitag H, Krueger A, Bauer S, Antelmann M, et al. Immunoadsorption to remove ß2 adrenergic receptor antibodies in Chronic Fatigue Syndrome CFS/ME. PLoS One. 2018;13(3):e0193672.
39. Cárdenas-Roldán J, Rojas-Villarraga A, Anaya JM. How do autoimmune diseases cluster in families? A systematic review and meta-analysis. BMC Med. 2013;11:73.
40. Niller HH, Wolf H, Ay E, Minarovits J. Epigenetic dysregulation of epstein-barr virus latency and development of autoimmune disease. Adv Exp Med Biol. 2011;711:82-102.
41. Janegova A, Janega P, Rychly B, Kuracinova K, Babal P. The role of Epstein-Barr virus infection in the development of autoimmune thyroid diseases. Endokrynol Pol. 2015;66(2):132-6.
42. Morris G, Maes M. A neuro-immune model of Myalgic Encephalomyelitis/Chronic fatigue syndrome. Metab Brain Dis. 2013;28(4):523-40.
43. Yáñez-Mó M, Siljander PR, Andreu Z, Zavec AB, Borràs FE, Buzas EI, et al. Biological properties of extracellular vesicles and their physiological functions. J Extracell Vesicles. 2015;4:27066.
44. Colombo M, Raposo G, Théry C. Biogenesis, Secretion, and Intercellular Interactions of Exosomes and Other Extracellular Vesicles. Annual Review of Cell and Developmental Biology. 2014;30(1):255-89.
45. Zaborowski MP, Balaj L, Breakefield XO, Lai CP. Extracellular Vesicles: Composition, Biological Relevance, and Methods of Study. Bioscience. 2015;65(8):783-97.
46. Théry C, Witwer KW, Aikawa E, Alcaraz MJ, Anderson JD, Andriantsitohaina R, et al. Minimal information for studies of extracellular vesicles 2018 (MISEV2018): a position statement of the International Society for Extracellular Vesicles and update of the MISEV2014 guidelines. Journal of Extracellular Vesicles. 2018;7(1):1535750.
47. van Niel G, D'Angelo G, Raposo G. Shedding light on the cell biology of extracellular vesicles. Nature Reviews Molecular Cell Biology. 2018;19(4):213-28.
48. Shah R, Patel T, Freedman JE. Circulating Extracellular Vesicles in Human Disease. New England Journal of Medicine. 2018;379(10):958-66.
49. Fitzgerald W, Freeman ML, Lederman MM, Vasilieva E, Romero R, Margolis L. A System of Cytokines Encapsulated in ExtraCellular Vesicles. Sci Rep. 2018;8(1):8973.
50. Mathieu M, Martin-Jaular L, Lavieu G, Théry C. Specificities of secretion and uptake of exosomes and other extracellular vesicles for cell-to-cell communication. Nat Cell Biol. 2019;21(1):9-17.
51. Bebelman MP, Smit MJ, Pegtel DM, Baglio SR. Biogenesis and function of extracellular vesicles in cancer. Pharmacol Ther. 2018;188:1-11.
52. Andreu Z, Yáñez-Mó M. Tetraspanins in extracellular vesicle formation and function. Front Immunol. 2014;5:442.
53. Couch Y, Buzàs EI, Di Vizio D, Gho YS, Harrison P, Hill AF, et al. A brief history of nearly EV-erything - The rise and rise of extracellular vesicles. J Extracell Vesicles. 2021;10(14):e12144.
54. ISEV. About the International Society for Extracellular Vesicles [January 13, 2023]. Available from: https://www.isev.org/about.
55. Lötvall J, Hill AF, Hochberg F, Buzás EI, Di Vizio D, Gardiner C, et al. Minimal experimental requirements for definition of extracellular vesicles and their functions: a position statement from the International Society for Extracellular Vesicles. J Extracell Vesicles. 2014;3:26913.
56. Lässer C, Jang SC, Lötvall J. Subpopulations of extracellular vesicles and their therapeutic potential. Mol Aspects Med. 2018;60:1-14.
57. Doyle LM, Wang MZ. Overview of Extracellular Vesicles, Their Origin, Composition, Purpose, and Methods for Exosome Isolation and Analysis. Cells. 2019;8(7).
58. Akers JC, Gonda D, Kim R, Carter BS, Chen CC. Biogenesis of extracellular vesicles (EV): exosomes, microvesicles, retrovirus-like vesicles, and apoptotic bodies. J Neurooncol. 2013;113(1):1-11.

59. Wickman G, Julian L, Olson MF. How apoptotic cells aid in the removal of their own cold dead bodies. Cell Death Differ. 2012;19(5):735-42.
60. Battistelli M, Falcieri E. Apoptotic Bodies: Particular Extracellular Vesicles Involved in Intercellular Communication. Biology (Basel). 2020;9(1).
61. Mateescu B, Kowal EJ, van Balkom BW, Bartel S, Bhattacharyya SN, Buzás EI, et al. Obstacles and opportunities in the functional analysis of extracellular vesicle RNA - an ISEV position paper. J Extracell Vesicles. 2017;6(1):1286095.
62. Heijnen HF, Schiel AE, Fijnheer R, Geuze HJ, Sixma JJ. Activated platelets release two types of membrane vesicles: microvesicles by surface shedding and exosomes derived from exocytosis of multivesicular bodies and alpha-granules. Blood. 1999;94(11):3791-9.
63. Mosquera-Heredia MI, Morales LC, Vidal OM, Barceló E, Silvera-Redondo C, Vélez JI, et al. Exosomes: Potential Disease Biomarkers and New Therapeutic Targets. Biomedicines. 2021;9(8).
64. Raposo G, Stoorvogel W, Strategic Infection B, dB, C I, Celbiologie-Algemeen LS, et al. Extracellular vesicles: Exosomes, microvesicles, and friends. J Cell Biol. 2013;200(4):373-83.
65. Abels ER, Breakefield XO. Introduction to Extracellular Vesicles: Biogenesis, RNA Cargo Selection, Content, Release, and Uptake. Cell Mol Neurobiol. 2016;36(3):301-12.
66. Stuffers S, Sem Wegner C, Stenmark H, Brech A. Multivesicular endosome biogenesis in the absence of ESCRTs. Traffic. 2009;10(7):925-37.
67. Tschuschke M, Kocherova I, Bryja A, Mozdziak P, Angelova Volponi A, Janowicz K, et al. Inclusion Biogenesis, Methods of Isolation and Clinical Application of Human Cellular Exosomes. J Clin Med. 2020;9(2).
68. Colombo M, Moita C, Van Niel G, Kowal J, Vigneron J, Benaroch P, et al. Analysis of ESCRT functions in exosome biogenesis, composition and secretion highlights the heterogeneity of extracellular vesicles. J Cell Sci. 2013;126(24):5553-65.
69. Gould SJ, Raposo G. As we wait: coping with an imperfect nomenclature for extracellular vesicles. Journal of Extracellular Vesicles. 2013;2(1):20389.
70. Simons M, Raposo G. Exosomes--vesicular carriers for intercellular communication. Curr Opin Cell Biol. 2009;21(4):575-81.
71. Menck K, Klemm F, Gross JC, Pukrop T, Wenzel D, Binder C. Induction and transport of Wnt 5a during macrophage-induced malignant invasion is mediated by two types of extracellular vesicles. Oncotarget. 2013;4(11):2057-66.
72. Mulcahy LA, Pink RC, Carter DR. Routes and mechanisms of extracellular vesicle uptake. J Extracell Vesicles. 2014;3.
73. Tóth E, Turiák L, Visnovitz T, Cserép C, Mázló A, Sódar BW, et al. Formation of a protein corona on the surface of extracellular vesicles in blood plasma. J Extracell Vesicles. 2021;10(11):e12140.
74. Cedervall T, Lynch I, Lindman S, Berggård T, Thulin E, Nilsson H, et al. Understanding the nanoparticle-protein corona using methods to quantify exchange rates and affinities of proteins for nanoparticles. Proc Natl Acad Sci U S A. 2007;104(7):2050-5.
75. Buzás EI, Tóth E, Sódar BW, Szabó-Taylor K. Molecular interactions at the surface of extracellular vesicles. Semin Immunopathol. 2018;40(5):453-64.
76. Johnstone RM, Adam M, Hammond JR, Orr L, Turbide C. Vesicle formation during reticulocyte maturation. Association of plasma membrane activities with released vesicles (exosomes). J Biol Chem. 1987;262(19):9412-20.
77. Valadi H, Ekström K, Bossios A, Sjöstrand M, Lee JJ, Lötvall JO. Exosome-mediated transfer of mRNAs and microRNAs is a novel mechanism of genetic exchange between cells. Nat Cell Biol. 2007;9(6):654-9.
78. Ratajczak J, Miekus K, Kucia M, Zhang J, Reca R, Dvorak P, et al. Embryonic stem cell-derived microvesicles reprogram hematopoietic progenitors: evidence for horizontal transfer of mRNA and protein delivery. Leukemia. 2006;20(5):847-56.
79. Skog J, Würdinger T, van Rijn S, Meijer DH, Gainche L, Sena-Esteves M, et al. Glioblastoma microvesicles transport RNA and proteins that promote tumour growth and provide diagnostic biomarkers. Nat Cell Biol. 2008;10(12):1470-6.

80. Escudé Martinez de Castilla P, Tong L, Huang C, Sofias AM, Pastorin G, Chen X, et al. Extracellular vesicles as a drug delivery system: A systematic review of preclinical studies. Adv Drug Deliv Rev. 2021;175:113801.
81. Hutcheson JD, Aikawa E. Extracellular vesicles in cardiovascular homeostasis and disease. Curr Opin Cardiol. 2018;33(3):290-7.
82. Eustes AS, Dayal S. The Role of Platelet-Derived Extracellular Vesicles in Immune-Mediated Thrombosis. Int J Mol Sci. 2022;23(14).
83. Raposo G, Nijman HW, Stoorvogel W, Liejendekker R, Harding CV, Melief CJ, et al. B lymphocytes secrete antigen-presenting vesicles. J Exp Med. 1996;183(3):1161-72.
84. Simon C, Greening DW, Bolumar D, Balaguer N, Salamonsen LA, Vilella F. Extracellular Vesicles in Human Reproduction in Health and Disease. Endocr Rev. 2018;39(3):292-332.
85. Buzas EI. The roles of extracellular vesicles in the immune system. Nature Reviews Immunology. 2023;23(4):236-50.
86. Pistono C, Bister N, Stanová I, Malm T. Glia-Derived Extracellular Vesicles: Role in Central Nervous System Communication in Health and Disease. Front Cell Dev Biol. 2020;8:623771.
87. Banks WA, Sharma P, Bullock KM, Hansen KM, Ludwig N, Whiteside TL. Transport of Extracellular Vesicles across the Blood-Brain Barrier: Brain Pharmacokinetics and Effects of Inflammation. Int J Mol Sci. 2020;21(12).
88. Delpech JC, Herron S, Botros MB, Ikezu T. Neuroimmune Crosstalk through Extracellular Vesicles in Health and Disease. Trends Neurosci. 2019;42(5):361-72.
89. Ciregia F, Urbani A, Palmisano G. Extracellular Vesicles in Brain Tumors and Neurodegenerative Diseases. Front Mol Neurosci. 2017;10:276.
90. Marcoux G, Laroche A, Hasse S, Bellio M, Mbarik M, Tamagne M, et al. Platelet EVs contain an active proteasome involved in protein processing for antigen presentation via MHC-I molecules. Blood. 2021;138(25):2607-20.
91. Clayton A, Mitchell JP, Court J, Linnane S, Mason MD, Tabi Z. Human tumor-derived exosomes down-modulate NKG2D expression. J Immunol. 2008;180(11):7249-58.
92. Mincheva-Nilsson L, Baranov V. Cancer exosomes and NKG2D receptor-ligand interactions: impairing NKG2D-mediated cytotoxicity and anti-tumour immune surveillance. Semin Cancer Biol. 2014;28:24-30.
93. Czystowska M, Han J, Szczepanski MJ, Szajnik M, Quadrini K, Brandwein H, et al. IRX-2, a novel immunotherapeutic, protects human T cells from tumor-induced cell death. Cell Death Differ. 2009;16(5):708-18.
94. Shinohara H, Kuranaga Y, Kumazaki M, Sugito N, Yoshikawa Y, Takai T, et al. Regulated Polarization of Tumor-Associated Macrophages by miR-145 via Colorectal Cancer-Derived Extracellular Vesicles. J Immunol. 2017;199(4):1505-15.
95. Costa-Silva B, Aiello NM, Ocean AJ, Singh S, Zhang H, Thakur BK, et al. Pancreatic cancer exosomes initiate pre-metastatic niche formation in the liver. Nat Cell Biol. 2015;17(6):816-26.
96. Lu M, DiBernardo E, Parks E, Fox H, Zheng SY, Wayne E. The Role of Extracellular Vesicles in the Pathogenesis and Treatment of Autoimmune Disorders. Front Immunol. 2021;12:566299.
97. Skriner K, Adolph K, Jungblut PR, Burmester GR. Association of citrullinated proteins with synovial exosomes. Arthritis Rheum. 2006;54(12):3809-14.
98. Cloutier N, Tan S, Boudreau LH, Cramb C, Subbaiah R, Lahey L, et al. The exposure of autoantigens by microparticles underlies the formation of potent inflammatory components: the microparticle-associated immune complexes. EMBO Mol Med. 2013;5(2):235-49.
99. Lee JY, Park JK, Lee EY, Lee EB, Song YW. Circulating exosomes from patients with systemic lupus erythematosus induce an proinflammatory immune response. Arthritis Res Ther. 2016;18(1):264.
100. FDA-NIH Biomarker Working Group BEST (Biomarkers, EndpointS, and other Tools) Resource: Silver Spring (MD): Food and Drug Administration (US); Bethesda (MD): National Institutes of Health (US); 2016 [Available from: https://www.ncbi.nlm.nih.gov/books/NBK326791/.
101. Califf RM. Biomarker definitions and their applications. Exp Biol Med (Maywood). 2018;243(3):213-21.

102. Hurwitz SN, Rider MA, Bundy JL, Liu X, Singh RK, Meckes DG, Jr. Proteomic profiling of NCI-60 extracellular vesicles uncovers common protein cargo and cancer type-specific biomarkers. Oncotarget. 2016;7(52):86999-7015.
103. Dhondt B, Geeurickx E, Tulkens J, Van Deun J, Vergauwen G, Lippens L, et al. Unravelling the proteomic landscape of extracellular vesicles in prostate cancer by density-based fractionation of urine. Journal of Extracellular Vesicles. 2020;9(1):1736935.
104. Danzer KM, Kranich LR, Ruf WP, Cagsal-Getkin O, Winslow AR, Zhu L, et al. Exosomal cell-to-cell transmission of alpha synuclein oligomers. Mol Neurodegener. 2012;7:42.
105. Puhm F, Boilard E, Machlus KR. Platelet Extracellular Vesicles: Beyond the Blood. Arterioscler Thromb Vasc Biol. 2021;41(1):87-96.
106. Motamedinia P, Scott AN, Bate KL, Sadeghi N, Salazar G, Shapiro E, et al. Urine Exosomes for Non-Invasive Assessment of Gene Expression and Mutations of Prostate Cancer. PLoS One. 2016;11(5):e0154507.
107. Thietart S, Rautou PE. Extracellular vesicles as biomarkers in liver diseases: A clinician's point of view. J Hepatol. 2020;73(6):1507-25.
108. Xu WC, Qian G, Liu AQ, Li YQ, Zou HQ. Urinary Extracellular Vesicle: A Potential Source of Early Diagnostic and Therapeutic Biomarker in Diabetic Kidney Disease. Chin Med J (Engl). 2018;131(11):1357-64.
109. Fiandaca MS, Kapogiannis D, Mapstone M, Boxer A, Eitan E, Schwartz JB, et al. Identification of preclinical Alzheimer's disease by a profile of pathogenic proteins in neurally derived blood exosomes: A case-control study. Alzheimers Dement. 2015;11(6):600-7.e1.
110. Gui Y, Liu H, Zhang L, Lv W, Hu X. Altered microRNA profiles in cerebrospinal fluid exosome in Parkinson disease and Alzheimer disease. Oncotarget. 2015;6(35):37043-53.
111. Palviainen M, Saraswat M, Varga Z, Kitka D, Neuvonen M, Puhka M, et al. Extracellular vesicles from human plasma and serum are carriers of extravesicular cargo-Implications for biomarker discovery. PLoS One. 2020;15(8):e0236439.
112. Veerman RE, Teeuwen L, Czarnewski P, Güclüler Akpinar G, Sandberg A, Cao X, et al. Molecular evaluation of five different isolation methods for extracellular vesicles reveals different clinical applicability and subcellular origin. J Extracell Vesicles. 2021;10(9):e12128.
113. Royo F, Théry C, Falcón-Pérez JM, Nieuwland R, Witwer KW. Methods for Separation and Characterization of Extracellular Vesicles: Results of a Worldwide Survey Performed by the ISEV Rigor and Standardization Subcommittee. Cells. 2020;9(9).
114. Livshits MA, Khomyakova E, Evtushenko EG, Lazarev VN, Kulemin NA, Semina SE, et al. Isolation of exosomes by differential centrifugation: Theoretical analysis of a commonly used protocol. Sci Rep. 2015;5:17319.
115. Li K, Wong DK, Hong KY, Raffai RL. Cushioned-Density Gradient Ultracentrifugation (C-DGUC): A Refined and High Performance Method for the Isolation, Characterization, and Use of Exosomes. Methods Mol Biol. 2018;1740:69-83.
116. Chen BY, Sung CW, Chen C, Cheng CM, Lin DP, Huang CT, et al. Advances in exosomes technology. Clin Chim Acta. 2019;493:14-9.
117. Böing AN, van der Pol E, Grootemaat AE, Coumans FA, Sturk A, Nieuwland R. Single-step isolation of extracellular vesicles by size-exclusion chromatography. J Extracell Vesicles. 2014;3.
118. Zeringer E, Barta T, Li M, Vlassov AV. Strategies for isolation of exosomes. Cold Spring Harb Protoc. 2015;2015(4):319-23.
119. Castro-Marrero J, Serrano-Pertierra E, Oliveira-Rodríguez M, Zaragozá MC, Martínez-Martínez A, Blanco-López MdC, et al. Circulating extracellular vesicles as potential biomarkers in chronic fatigue syndrome/myalgic encephalomyelitis: an exploratory pilot study. Journal of Extracellular Vesicles. 2018;7(1):1453730.
120. Almenar-Pérez E, Sarría L, Nathanson L, Oltra E. Assessing diagnostic value of microRNAs from peripheral blood mononuclear cells and extracellular vesicles in Myalgic Encephalomyelitis/Chronic Fatigue Syndrome. Sci Rep. 2020;10(1):2064.
121. Eguchi A, Fukuda S, Kuratsune H, Nojima J, Nakatomi Y, Watanabe Y, et al. Identification of actin network proteins, talin-1 and filamin-A, in circulating extracellular vesicles as blood biomarkers

for human myalgic encephalomyelitis/chronic fatigue syndrome. Brain, Behavior, and Immunity. 2020;84:106-14.
122. Giloteaux L, O'Neal A, Castro-Marrero J, Levine SM, Hanson MR. Cytokine profiling of extracellular vesicles isolated from plasma in myalgic encephalomyelitis/chronic fatigue syndrome: a pilot study. J Transl Med. 2020;18(1):387.
123. Bonilla H, Hampton D, Marques de Menezes EG, Deng X, Montoya JG, Anderson J, et al. Comparative Analysis of Extracellular Vesicles in Patients with Severe and Mild Myalgic Encephalomyelitis/Chronic Fatigue Syndrome. Front Immunol. 2022;13:841910.
124. Tsilioni I, Natelson B, Theoharides TC. Exosome-associated mitochondrial DNA from patients with myalgic encephalomyelitis/chronic fatigue syndrome stimulates human microglia to release IL-1β. Eur J Neurosci. 2022;56(10):5784-94.
125. González-Cebrián A, Almenar-Pérez E, Xu J, Yu T, Huang WE, Giménez-Orenga K, et al. Diagnosis of Myalgic Encephalomyelitis/Chronic Fatigue Syndrome With Partial Least Squares Discriminant Analysis: Relevance of Blood Extracellular Vesicles. Front Med (Lausanne). 2022;9:842991.
126. Sellam J, Proulle V, Jüngel A, Ittah M, Miceli Richard C, Gottenberg JE, et al. Increased levels of circulating microparticles in primary Sjögren's syndrome, systemic lupus erythematosus and rheumatoid arthritis and relation with disease activity. Arthritis Res Ther. 2009;11(5):R156.
127. Lee J-H, Ostalecki C, Oberstein T, Schierer S, Zinser E, Eberhardt M, et al. Alzheimer's disease protease-containing plasma extracellular vesicles transfer to the hippocampus via the choroid plexus. eBioMedicine. 2022;77:103903.
128. OUS. Tematisk forskningsbiobank og register for CFS/ME 2021 [March 26th 2023]. Available from: https://oslo-universitetssykehus.no/personvern/informasjonsportal-for-deg-som-har-avgitt-bredt-samtykke/tematisk-forskningsbiobank-og-register-for-cfsme#om-cfsme-biobank-og-register.
129. Izon Science Ltd. AFC(V1) User Manual [Available from: https://support.izon.com/afc-user-manual.
130. Izon Science Ltd. What is the latest version of AFC(V1) firmware? [Available from: https://support.izon.com/what-is-the-latest-version-of-afc-software.
131. Mahmood T, Yang PC. Western blot: technique, theory, and trouble shooting. N Am J Med Sci. 2012;4(9):429-34.
132. Alegria-Schaffer A. Western blotting using chemiluminescent substrates. Methods Enzymol. 2014;541:251-9.
133. Harris JR. Transmission electron microscopy in molecular structural biology: A historical survey. Arch Biochem Biophys. 2015;581:3-18.
134. Théry C, Amigorena S, Raposo G, Clayton A. Isolation and characterization of exosomes from cell culture supernatants and biological fluids. Curr Protoc Cell Biol. 2006;Chapter 3:Unit 3.22.
135. Dragovic RA, Gardiner C, Brooks AS, Tannetta DS, Ferguson DJ, Hole P, et al. Sizing and phenotyping of cellular vesicles using Nanoparticle Tracking Analysis. Nanomedicine. 2011;7(6):780-8.
136. Mellon FA. MASS SPECTROMETRY | Principles and Instrumentation. In: Caballero B, editor. Encyclopedia of Food Sciences and Nutrition (Second Edition). Oxford: Academic Press; 2003. p. 3739-49.
137. Vogeser M, Parhofer KG. Liquid chromatography tandem-mass spectrometry (LC-MS/MS)--technique and applications in endocrinology. Exp Clin Endocrinol Diabetes. 2007;115(9):559-70.
138. Oslo University Hospital. Welcome to: The Proteomics Core Facility (PCF) at Oslo University Hospital [Available from: https://www.ous-research.no/proteomics/.
139. ggplot2: Elegant Graphics for Data Analysis [Internet]. Springer-Verlag New York. 2016. Available from: https://ggplot2.tidyverse.org.
140. ggpubr: 'ggplot2' Based Publication Ready Plots [Internet]. 2023. Available from: https://rpkgs.datanovia.com/ggpubr/.
141. Kalra H, Simpson RJ, Ji H, Aikawa E, Altevogt P, Askenase P, et al. Vesiclepedia: a compendium for extracellular vesicles with continuous community annotation. PLoS Biol. 2012;10(12):e1001450.

142. Coumans FAW, Brisson AR, Buzas EI, Dignat-George F, Drees EEE, El-Andaloussi S, et al. Methodological Guidelines to Study Extracellular Vesicles. Circ Res. 2017;120(10):1632-48.
143. Stranska R, Gysbrechts L, Wouters J, Vermeersch P, Bloch K, Dierickx D, et al. Comparison of membrane affinity-based method with size-exclusion chromatography for isolation of exosome-like vesicles from human plasma. J Transl Med. 2018;16(1):1.
144. Monguió-Tortajada M, Gálvez-Montón C, Bayes-Genis A, Roura S, Borràs FE. Extracellular vesicle isolation methods: rising impact of size-exclusion chromatography. Cell Mol Life Sci. 2019;76(12):2369-82.
145. Zhang X, Takeuchi T, Takeda A, Mochizuki H, Nagai Y. Comparison of serum and plasma as a source of blood extracellular vesicles: Increased levels of platelet-derived particles in serum extracellular vesicle fractions alter content profiles from plasma extracellular vesicle fractions. PLoS One. 2022;17(6):e0270634.
146. Maroto R, Zhao Y, Jamaluddin M, Popov VL, Wang H, Kalubowilage M, et al. Effects of storage temperature on airway exosome integrity for diagnostic and functional analyses. J Extracell Vesicles. 2017;6(1):1359478.
147. Gardiner C, Ferreira YJ, Dragovic RA, Redman CW, Sargent IL. Extracellular vesicle sizing and enumeration by nanoparticle tracking analysis. J Extracell Vesicles. 2013;2.
148. Nakatomi Y, Mizuno K, Ishii A, Wada Y, Tanaka M, Tazawa S, et al. Neuroinflammation in Patients with Chronic Fatigue Syndrome/Myalgic Encephalomyelitis: An ^{11}C-(R)-PK11195 PET Study. J Nucl Med. 2014;55(6):945-50.
149. Vestad B, Nyman TA, Hove-Skovsgaard M, Stensland M, Hoel H, Trøseid AS, et al. Plasma extracellular vesicles in people living with HIV and type 2 diabetes are related to microbial translocation and cardiovascular risk. Sci Rep. 2021;11(1):21936.
150. Rydland A, Heinicke F, Flåm ST, Mjaavatten MD, Lie BA. Small extracellular vesicles have distinct CD81 and CD9 tetraspanin expression profiles in plasma from rheumatoid arthritis patients. Clin Exp Med. 2023.
151. Begum H, Murugesan P, Tangutur AD. Western blotting: a powerful staple in scientific and biomedical research. BioTechniques. 2022;73(1):58-69.
152. Mørk M, Handberg A, Pedersen S, Jørgensen MM, Bæk R, Nielsen MK, et al. Prospects and limitations of antibody-mediated clearing of lipoproteins from blood plasma prior to nanoparticle tracking analysis of extracellular vesicles. J Extracell Vesicles. 2017;6(1):1308779.
153. Van Niel G, Raposo G, Candalh C, Boussac M, Hershberg R, Cerf–Bensussan N, et al. Intestinal epithelial cells secrete exosome–like vesicles. Gastroenterology. 2001;121(2):337-49.
154. Borges FT, Melo SA, Özdemir BC, Kato N, Revuelta I, Miller CA, et al. TGF-β1–Containing Exosomes from Injured Epithelial Cells Activate Fibroblasts to Initiate Tissue Regenerative Responses and Fibrosis. J Am Soc Nephrol. 2013;24(3):385-92.
155. van der Pol E, Coumans FA, Grootemaat AE, Gardiner C, Sargent IL, Harrison P, et al. Particle size distribution of exosomes and microvesicles determined by transmission electron microscopy, flow cytometry, nanoparticle tracking analysis, and resistive pulse sensing. J Thromb Haemost. 2014;12(7):1182-92.
156. Vestad B, Llorente A, Neurauter A, Phuyal S, Kierulf B, Kierulf P, et al. Size and concentration analyses of extracellular vesicles by nanoparticle tracking analysis: a variation study. J Extracell Vesicles. 2017;6(1):1344087.
157. Noren Hooten N, Byappanahalli AM, Vannoy M, Omoniyi V, Evans MK. Influences of age, race, and sex on extracellular vesicle characteristics. Theranostics. 2022;12(9):4459-76.
158. Nederveen JP, Warnier G, Di Carlo A, Nilsson MI, Tarnopolsky MA. Extracellular Vesicles and Exosomes: Insights From Exercise Science. Front Physiol. 2020;11:604274.
159. Sódar BW, Kittel Á, Pálóczi K, Vukman KV, Osteikoetxea X, Szabó-Taylor K, et al. Low-density lipoprotein mimics blood plasma-derived exosomes and microvesicles during isolation and detection. Sci Rep. 2016;6:24316.
160. Hart A. Mann-Whitney test is not just a test of medians: differences in spread can be important. BMJ. 2001;323(7309):391-3.
161. Hornig M, Montoya JG, Klimas NG, Levine S, Felsenstein D, Bateman L, et al. Distinct plasma immune signatures in ME/CFS are present early in the course of illness. Sci Adv. 2015;1(1).

Appendix 1. Antibodies

Supplementary table 1: Antibodies utilized in western blot and immuno-transmission electron microscopy.

Use	**Target**	**Antibody (clone)**	**Host species**	**Supplier (headquarters)**	**Catalog number**
Western blot	CD9	CD9 Monoclonal Antibody (Ts9)	Mouse	Invitrogen (Waltham, MA, USA)	10626D
	CD63	CD63 Monoclonal Antibody (Ts63)	Mouse	Invitrogen (Waltham, MA, USA)	10628D
	TSG101	TSG101 Monoclonal Antibody (4A10)	Mouse	Invitrogen (Waltham, MA, USA)	MA1-23296
	Albumin	ALB Monoclonal Antibody (F-10)	Mouse	Santa Cruz Biotechnology (Santa Cruz, CA, USA)	sc-271605
	Mouse derived primary antibody	Anti-mouse IgG, HRP-linked Antibody	Horse	Cell Signaling Technology (Danvers, MA, USA)	7076
Western blot optimization, exclusively	CD9	CD9 Monoclonal Antibody (C-4)	Mouse	Santa Cruz Biotechnology (Santa Cruz, CA, USA)	sc-13118
	CD81	CD81 Monoclonal antibody (B-11)	Mouse	Santa Cruz Biotechnology (Santa Cruz, CA,	sc-166029

				USA)	
Transmission electron microscopy	CD63	CD63 LAMP-3	Mouse	Developmental Studies Hybridoma Bank, University of Iowa (Iowa city, IA, USA)	H5C6
	Mouse derived primary antibody	AffiniPure Rabbit Anti-Mouse	Rabbit	Jackson Immunoresearch (Cambridge, UK)	315-005-044

Appendix 2. Software

Excel was used to view and manage data. FunRich was used to analyze proteomics data. ImageQuant software was used to operate the imaging of western blots and create multiplex images. R was used to analyze clinical data, EV characteristics data, and proteomics data.

Supplementary table 2: Softwares used for the work presented in thesis.

Software	**Version**
Excel	**2211**
FunRich	3.1.3
ImageQuant LAS 4000	1.2
ImageQuant TL	8.1.0.0
R	4.2.0
RStudio	2022.02.2+485

Appendix 3. Histograms and Q-Q plots of NTA data

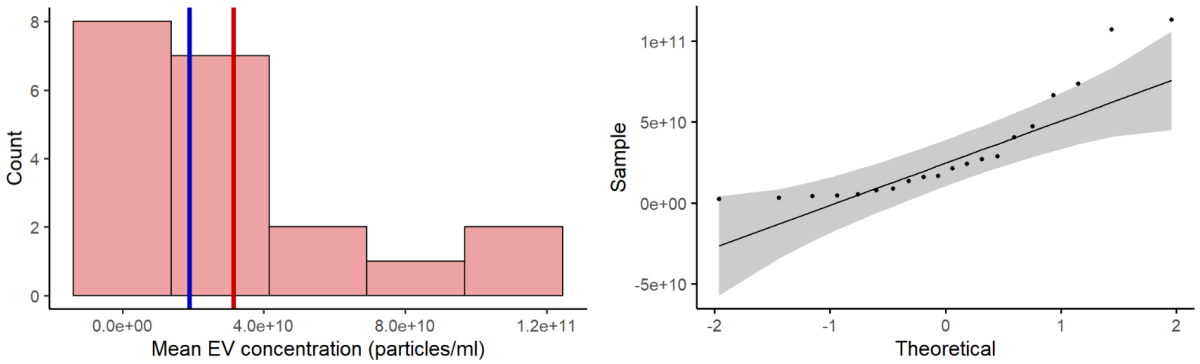

Supplementary figure 1: Histogram and quantile-quantile plot of mean EV concentration in the ME/CFS cohort (n=20). *The red line indicates the mean, and the blue the median.*

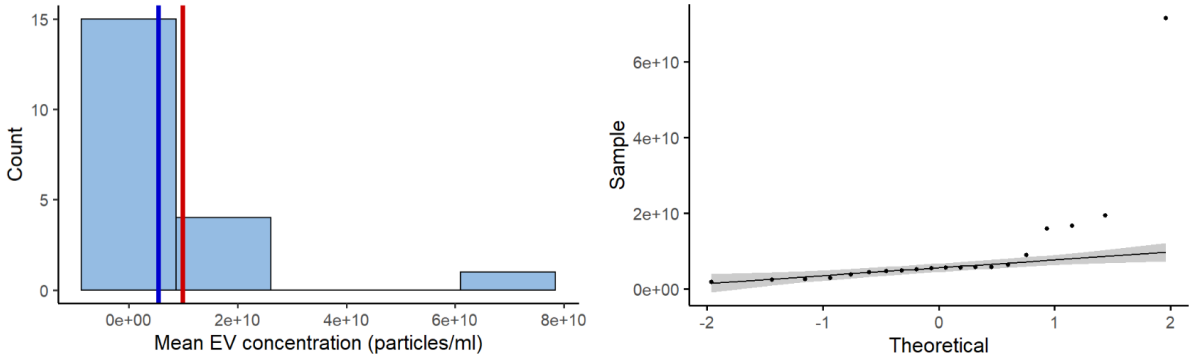

Supplementary figure 2: Histogram and quantile-quantile plot of mean EV concentration in the HC cohort (n=20). *The red line indicates the mean, and the blue the median.*

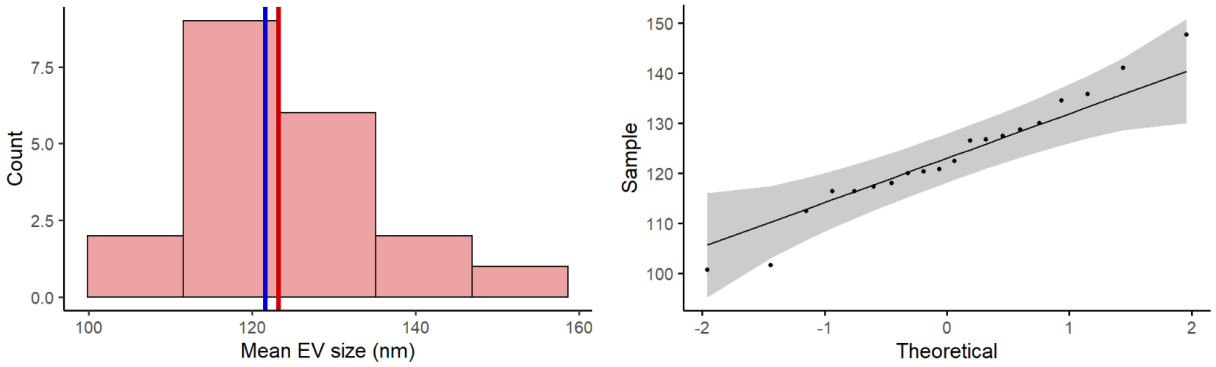

Supplementary figure 3: Histogram and quantile-quantile plot of mean EV size in the ME/CFS cohort (n=20). *The red line indicates the mean, and the blue the median.*

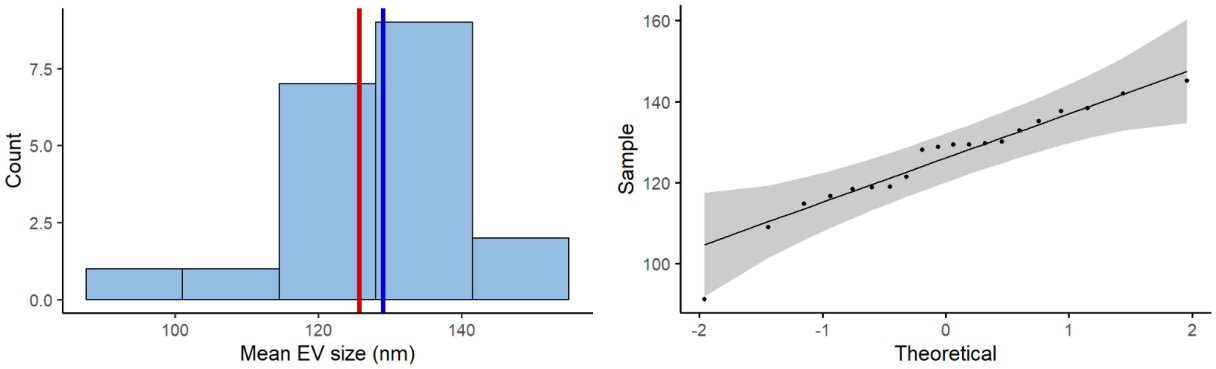

Supplementary figure 4: Histogram and quantile-quantile plot of mean EV size in the HC cohort (n=20)*. The red line indicates the mean, and the blue the median.*

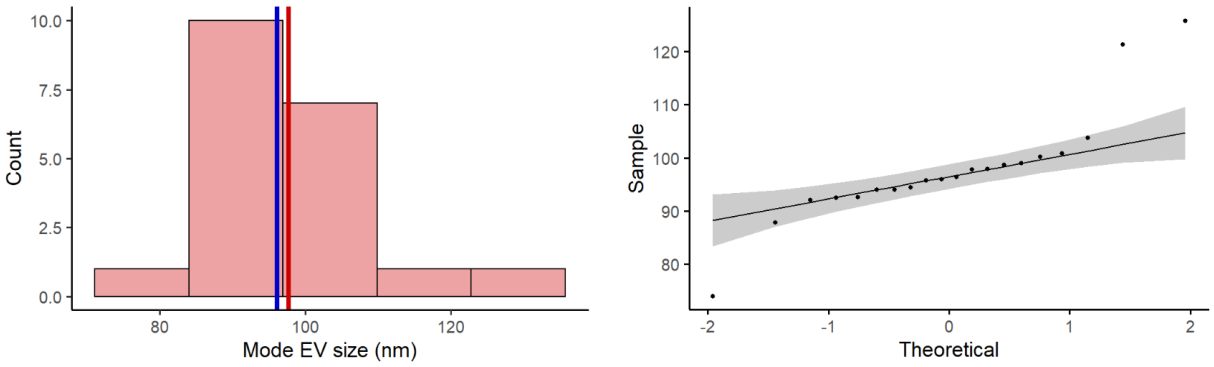

Supplementary figure 5: Histogram and quantile-quantile plot of mode EV size in the ME/CFS cohort (n=20). *The red line indicates the mean, and the blue the median.*

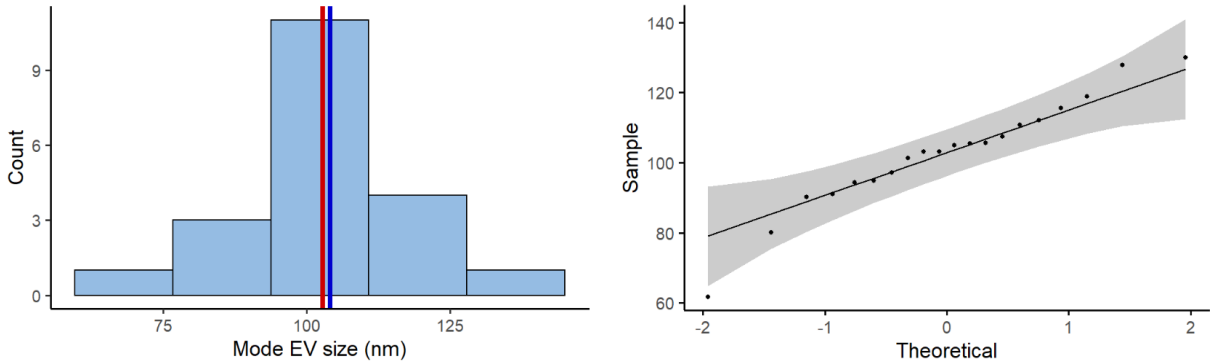

Supplementary figure 6: Histogram and quantile-quantile plot of mode EV size in the ME/CFS cohort (n=20). *The red line indicates the mean, and the blue the median.*